1876

Y-1487
Engineering & Equipment

AEC RESEARCH AND DEVELOPMENT REPORT

MASTER

ISOSTATIC HOT PRESSING

R. P. Levey

UNION CARBIDE CORPORATION
NUCLEAR DIVISION
OAK RIDGE Y-12 PLANT

operated for the ATOMIC ENERGY COMMISSION *under* U. S. GOVERNMENT Contract W-7405 eng 26

UNION CARBIDE

OAK RIDGE Y-12 PLANT
P. O. Box Y
OAK RIDGE, TENNESSEE 37831

DISCLAIMER

Printed in USA. Price $3.00. Available from the Clearinghouse for Federal Scientific and Technical Information, National Bureau of Standards, U.S. Department of Commerce, Springfield, Virginia

Date Issued: December 30, 1965

Report Number Y-1487

Engineering and Equipment
TID-4500 (45th Edition)

UNION CARBIDE CORPORATION
Nuclear Division

Y-12 PLANT

Contract W-7405-eng-26
With the US Atomic Energy Commission

ISOSTATIC HOT PRESSING

R. P. Levey

Oak Ridge, Tennessee
June 9, 1965

Report Number Y-1487

Engineering and Equipment
TID-4500 (45th Edition)

Distribution:

Ackerson, R. D.	(AFSC)	Keller, C. A.	(AEC-ORO)(4)
Ballenger, H. F.	(2)	Kite, H. T.	
Briscoe, O. W.		Lewis, F. O.	(ORGDP)
Burkhart, L. E.		McLendon, J. D.	
Center, C. E.	(ORGDP)	Mitchel, G. W.	
Christman, A. M.		Patton, F. S.	
Cowen, D. D.	(ORNL)	Waters, J. L.	
Dow, Neal		Whitson, W. K.	
Fortenbery, M. J.		Winkel, R. A.	(Paducah)
Harwell, W. L.	(ORGDP)(5)	Zurcher, E.	
Hemphill, L. F.		Y-12 Central Files	(5)
Huber, A. P.	(ORGDP)	Y-12 Central Files	(Y-12RC)
Huddleston, R. L.	(15)		

In addition, this report is distributed in accordance with the category Engineering and Equipment, as given in the "USAEC Standard Distribution Lists for Unclassified Scientific and Technical Reports", TID-4500 (45th Edition), September 1, 1965.

ABSTRACT

An isostatic hot-pressing system has been developed at 15,000 to 30,000 psi for large compacts. Process demonstrations have illustrated the practicality of the system with eight-inch-diameter bars at 2000° C and twelve-inch-diameter bars at 1200° C. Furthermore, the data indicate that a modification of the existing equipment will provide capacity to forty inches in diameter at 2500° C and 30,000 psi.

THIS PAGE

WAS INTENTIONALLY

LEFT BLANK

CONTENTS

THIS PAGE

WAS INTENTIONALLY

LEFT BLANK

INTRODUCTION

Hydrostatic pressing techniques, although known and practiced on a small scale in laboratories prior to World War II, did not find large-scale and commercial usage until recently. Newkirk and Anicetti[1] have described the development and salient features of this technique in some detail. The particular advantage over the older die or punch-forming method lies in the fact that a relatively stress-free body of higher green strength and density results at any given forming pressure. In addition, complex shapes are readily produced. Sinters made from hydrostatically formed parts are inherently stronger in the transverse direction.

About 1950, Y-12 began hydrostatic pressing operations and since then has developed the technique to a high degree. During this period a complex of hydrostatic facilities has become available for work to 30,000 psi. Pressings up to 58 inches in diameter and 56 inches long or 28 inches in diameter and 96 inches long can be handled. Concurrent with these developments in hydrostatic pressing, limitations in hot-pressing techniques make it desirable to provide the isostatic press with the simultaneous application of heat. Hot pressing has been traditionally accomplished in graphite dies. Although there are no particular temperature limitations, pressures above 3000 psi cannot be sustained. High-temperature metal dies of super alloys have been constructed which are capable of pressures of 10,000 psi at 1000° C. However, the sintering temperatures required for refractory metals and oxides are generally above 1700° C. Thus, in situations where a pressure of 3000 psi is insufficient, there are no forming techniques available beyond the traditional cold press-sintering cycle.

A rapidly developing technique for the simultaneous application of heat and isostatic pressure is the gas autoclave, a system that employs a pressure vessel into which is built a furnace. The furnace, in turn, contains the part to be sintered under pressure, and cooling is provided to protect the vessel from furnace heat. The system is pressured with gas while the part, when open voids are present, is sealed by proper canning. Battelle Laboratories[2 - 4] began developing gas autoclaves for pressure-bonding work but have expanded the interest to include pressure sintering. Although the value of this technique is obvious, there are prodigious technological difficulties to resolve before it may be used on an industrial scale. These problems have been discussed by Muzzall[5] and principally involve the difficulties and hazards in compressing and handling large volumes of gas. In addition, when pressing powder masses at high temperatures, a can or other refractory container must be provided which is absolutely leak tight under the existing conditions of deformation, temperature, and pressure. Thus, when a certain volume of powder is canned to provide 50% voidage and pressed to 15,000 psi and the necessary temperature so that the powder resistance to motion is nil, the density cannot exceed 98% of theoretical simply because the initially trapped gas occupies this volume at equilibrium. The production of weldments in refractory metals sufficiently tight and homogeneous

to withstand the required distortions has not yet been demonstrated and remains a major difficulty in gas-autoclave methods.

As previously described, the gas-autoclave method of hot isostatic pressing is presently enjoying rapid growth and expanding application. The major difficulties are concerned with the characteristically long pressurization and heating cycles together with the extensive equipment required for gas compression, purification, and storage. In addition to the problem of effectual canning, the technique is currently both expensive and hazardous.

One method of accomplishing the hot press in solid media has been developed at Y-12. The operation employs conventional graphite dies filled with graphite powder. The part to be pressed is buried in the powder and pressed. Since the specimen pressure is applied through a powder medium, it is more uniform than if directly applied from a piston. The efficiency of pressure generation in the radial direction has not been studied. The ceiling pressure available is about 3000 psi.

This present work accomplishes the hot press in a sand medium under vacuum. The problems common to the gas autoclave, namely gas compression, handling, canning, and operational hazards are thus avoided. The sand medium is compressed by oil using existing equipment ordinarily or otherwise employed for cold isostatic pressing. The concept of an internal furnace containing a specimen compressed by secondary media is not new. University and other small research devices requiring heat and ultra high pressure generally depend upon similar arrangements. For example, Hall[6-8] describes several configurations in which a specimen and heating element are compressed by a pyrophyllite secondarily driven to pressure. He reports attaining pressures of 1.5 million psi at 3000° C. There is a generic relationship between such a research apparatus and the equipment involved in this present work. For operational application, however, the design and development problems come, primarily, from the scale of operations. The sand-pressing developments described have been limited to the following:

1. Demonstration of the isostatic pressure transmission in the chosen sand.

2. Development of an operational containment system for the sand.

3. Development of an improved sand-containment device.

4. A cost analysis of operations on the 17 and 27-inch-diameter scale.

5. A forecast of the capability and power requirements that are required for full exploitation of the Y-12 sixty-inch-diameter isostat.

SUMMARY

This report describes the development of an isostatic hot-pressing system for operational usage on an unprecedented scale.

The pressing is accomplished by high-pressure oil or water acting on a directly heated specimen via a sand medium that is inert, insulating, nonforming, and pressure transmitting. Temperatures to 3000° C can be readily obtained and an operating pressure of 15,000 psi has been employed throughout the study. All the equipment used, however, is rated for an operational level of 30,000 psi.

In the course of this development, the isotropic nature of sand pressure transmission has been shown and a simple, inexpensive, disposable, refractory metal furnace has been evolved. In detailing the evolution of the pressing system, some 24 successive pressings were accomplished without a single case of leakage. The steady-state power, specimen temperature, and specimen size data have been fitted to a simple model. The results are applied to the 60-inch-diameter vessel to fully realize its potential in this work. Results indicate that a 1000-kw power supply will permit 42-inch-diameter by 42-inch-long bars to be pressed at 2500° C.

THIS PAGE

WAS INTENTIONALLY

LEFT BLANK

DESCRIPTION OF THE EXPERIMENTS

EXPERIMENTAL EQUIPMENT

Pressure Vessel

The pilot-scale runs were all accomplished in a vessel made from a war-surplus 16-inch naval gun. After shortening it and removing the rifling, a work hole was obtained that measures 17 inches in diameter and 144 inches deep. The gun was mounted vertically with the breech at the top. This breech is of an interrupted buttress thread design with a well-contoured lead in and can be hydraulically swung 90 degrees upward to give clear access to the vessel. The vessel bottom is provided with a continuous thread and retainer. The upper and lower seals, called mushrooms, are provided with Bridgeman-type seals having an ~ 3% unsupported area. A sectional view of the vessel is presented in Figures 1 through 3. The entire assembly is located in a concrete bunker with access both upstairs and down through steel-plate sliding doors. The bunker contains all the high-pressure equipment such as lines, pumps, and valves. The valves, called dump valves, are pneumatically actuated from outside the bunker at the control panel.

Feedthroughs

Prior to the hot-pressing project, the refurbished gun was used in cold isostatic pressing studies. The vessel was used regularly at 30,000 psi and tested occasionally to 45,000 psi. However, the mushrooms were designed only with sealing in mind; not with a view to providing an entrance through it to pass in power and instrument leads. The usable feedthrough space is confined to a three-inch-diameter column in the bottom mushroom, shown schematically in Figure 3.

For hot-pressing studies it was considered desirable to provide an entrance for twelve instrument leads and twelve 1000-ampere single-phase power leads. It was also agreed that the mushroom forging had sufficient value to require that the feedthrough be installed in the existing part. Accordingly, a 2 1/2-inch-diameter hole was bored through the mushroom nose (~ 3" D). In the hole, four 3/4-inch-diameter copper power leads, a 3/4-inch-diameter stainless steel oil feed pipe, and twelve 16-gauge instrument leads were set in a convenient pattern and retained under tension.

After scrupulous cleaning, the hole was potted with epoxy resin to a depth of about two feet. This amount was considered adequate after studying the data from sample pottings at various lengths in 1/4-inch-diameter pipe that were tested to failure. A plastic-metal shear strength of 1200 psi was taken for design purposes. The load rating of a given potting is approximated by:

$$p = 4 (R)\ 1/d,$$

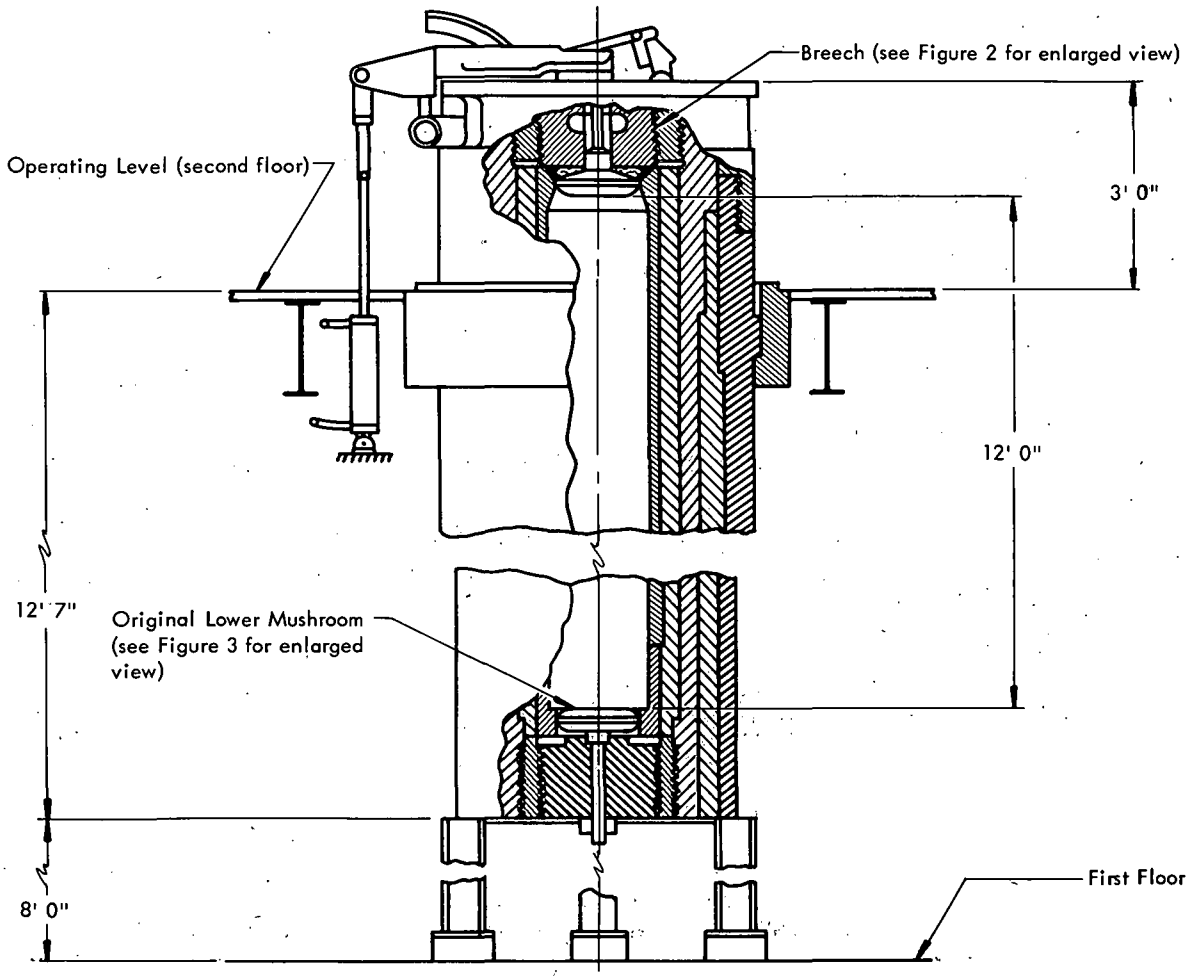

Figure 1. SIXTEEN-INCH PRESSURE VESSEL.

where:

p represents the failure pressure in psi,

R the resin-metal bond shear strength in psi, and

1/d the aspect ratio of the potting.

This equation predicts a failure load of over 46,000 psi for the seal. However, the first feedthrough failed under 5000 psi. A second attempt was made along the same lines except that all surfaces to be potted were first carefully given a one to three-mil coating of plastic and cured to make certain a good bond was attained. The potting was then done in stages to minimize the stresses that arise from volumetric shrinkage during the cure. Despite these efforts, the second seal failed at about the same pressure—slightly above 5000 psi.

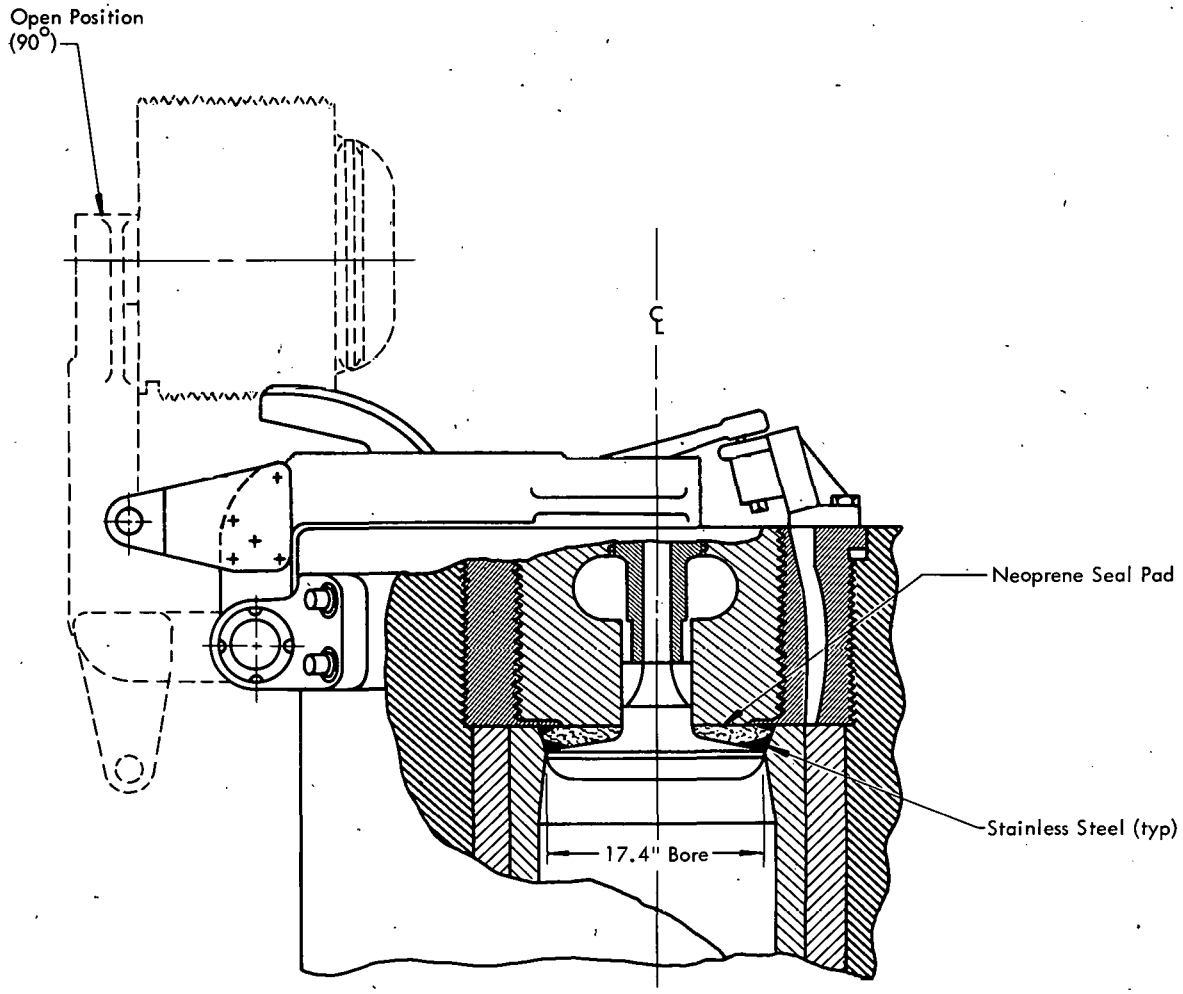

Figure 2. ENLARGED VIEW OF THE BREECH ON THE SIXTEEN-INCH PRESSURE VESSEL.

A redesign of the feedthrough was now undertaken as shown in Figure 4. The lower mushroom was modified to take a hardened Type AISI 4340 stainless steel thrust tube containing the sealed leads as shown. In this design the actual thrust is absorbed on machined surfaces while an oil seal is accomplished by a thin fusion weld as indicated. The high-strength steel thrust tube was tapered inside to resist plastic extrusion. In addition, the tube was grooved the entire length to enhance the bonding and prevent slippage. Finally, a hardened steel load block and retainer were provided. This assembly alone could conservatively support the resin column in the absence of any bond at all. (The thrust tube load at a 30,000-psi vessel pressure is 93 tons.) The oil tube and copper bus bars were given a knurled finish. All parts were coated with plastic in advance and cured before potting. The final potting was done in three steps. The resin used was Z-cured Shell Epon 828. After installation, the seal was tested to 40,000 psi without leakage. The unit has now seen over two years of uninterrupted service.

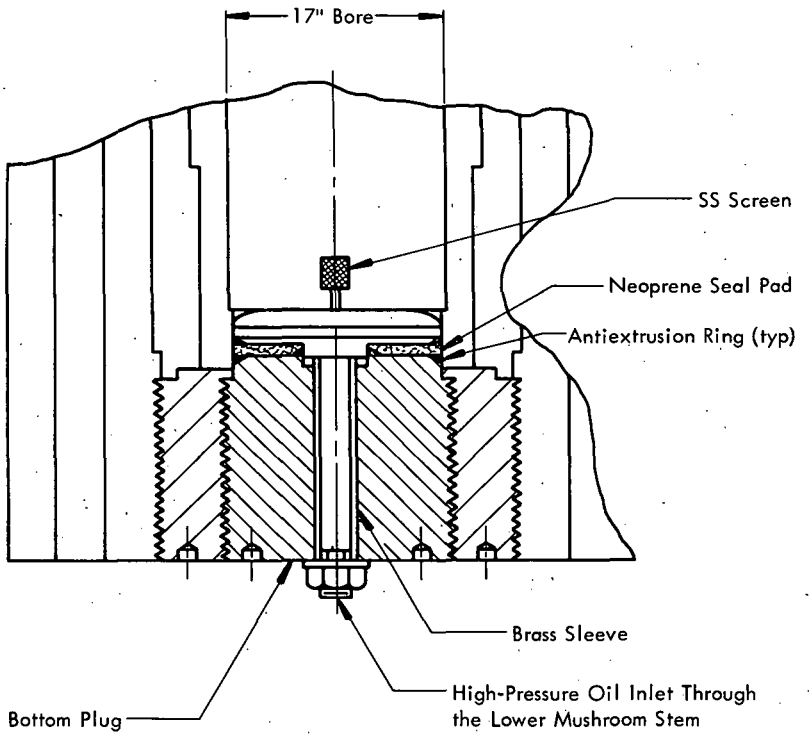

Figure 3. ENLARGED VIEW OF THE ORIGINAL LOWER MUSHROOM OF THE SIXTEEN-INCH PRESSURE VESSEL.

Vessel Piping and Auxiliaries

A piping schematic of the pilot vessel is presented in Figure 5 along with the important pressure piping. The vessel pressure is derived from an intensifier[a] that is a double-ended device with a 10-inch-diameter primary piston and 1 3/8-inch-diameter high-pressure pistons. The machine has a pumping speed of 3/4 gal/min at 30,000 psi.

The vessel is normally filled or emptied using flexible hose and a service pump. The full vessel is closed and bled of gas using a 1 1/2-gpm gear pump and a bleed valve. The room is then sealed off and the high-pressure pump started. After pressing, the pressure is reduced through the top dump valve and into a separate tank system outside the building for protection against flammable gas release.

Instruments and Electrical System

The electrical arrangement is shown in Figure 6. Ten to 12 kilowatts at the furnace are available depending upon how closely matched are the filament and power supply. Incoming 440-volt power fused at 50 amperes is 100% manually variable with an autotransformer rated at 30 amperes. The power is monitored by an integrating

(a) Harwood Engineering Company Model DA-10.

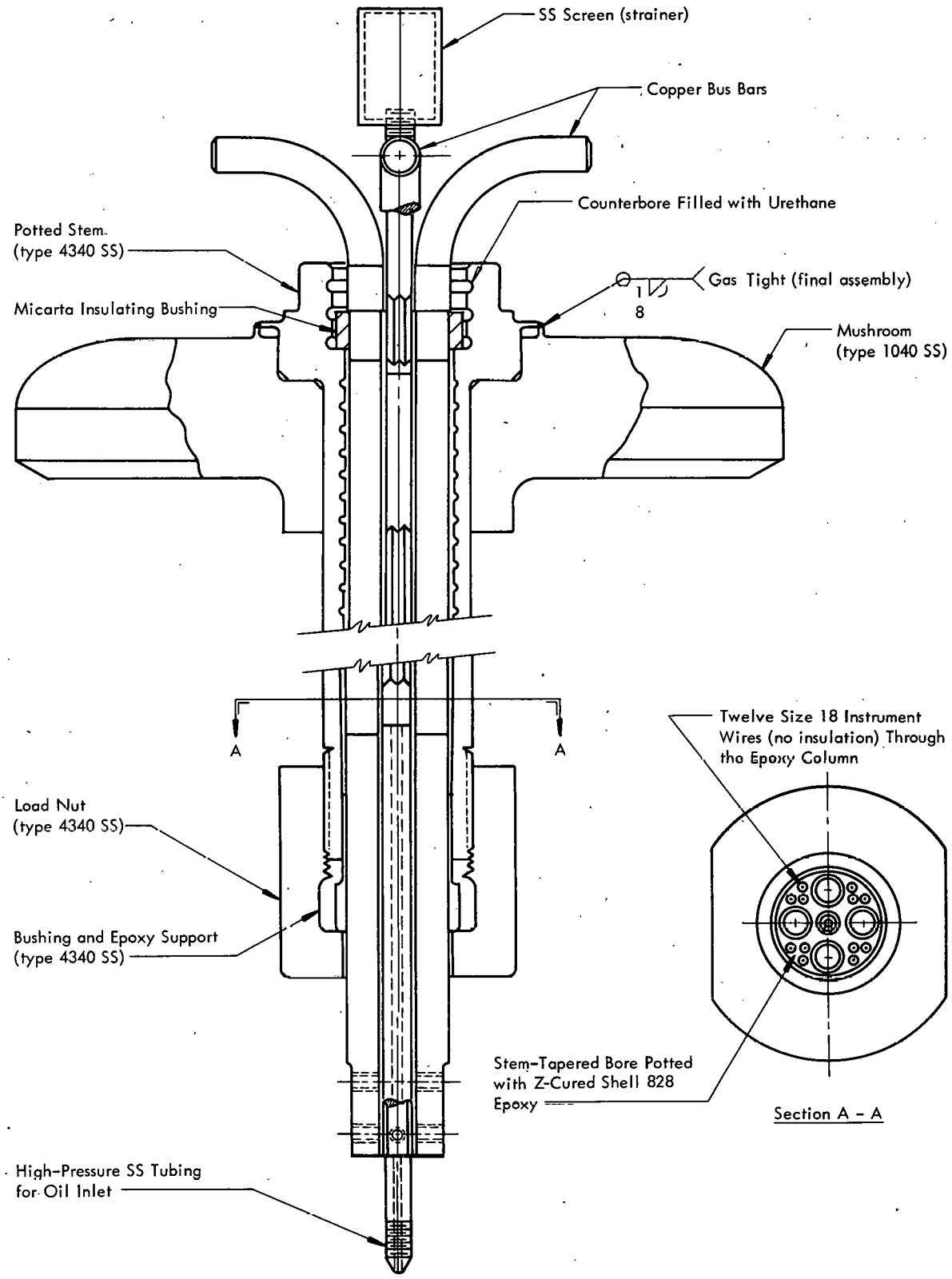

Figure 4. REVISED SIXTEEN-INCH LOWER MUSHROOM WITH POWER SUPPLY FEEDTHROUGH.

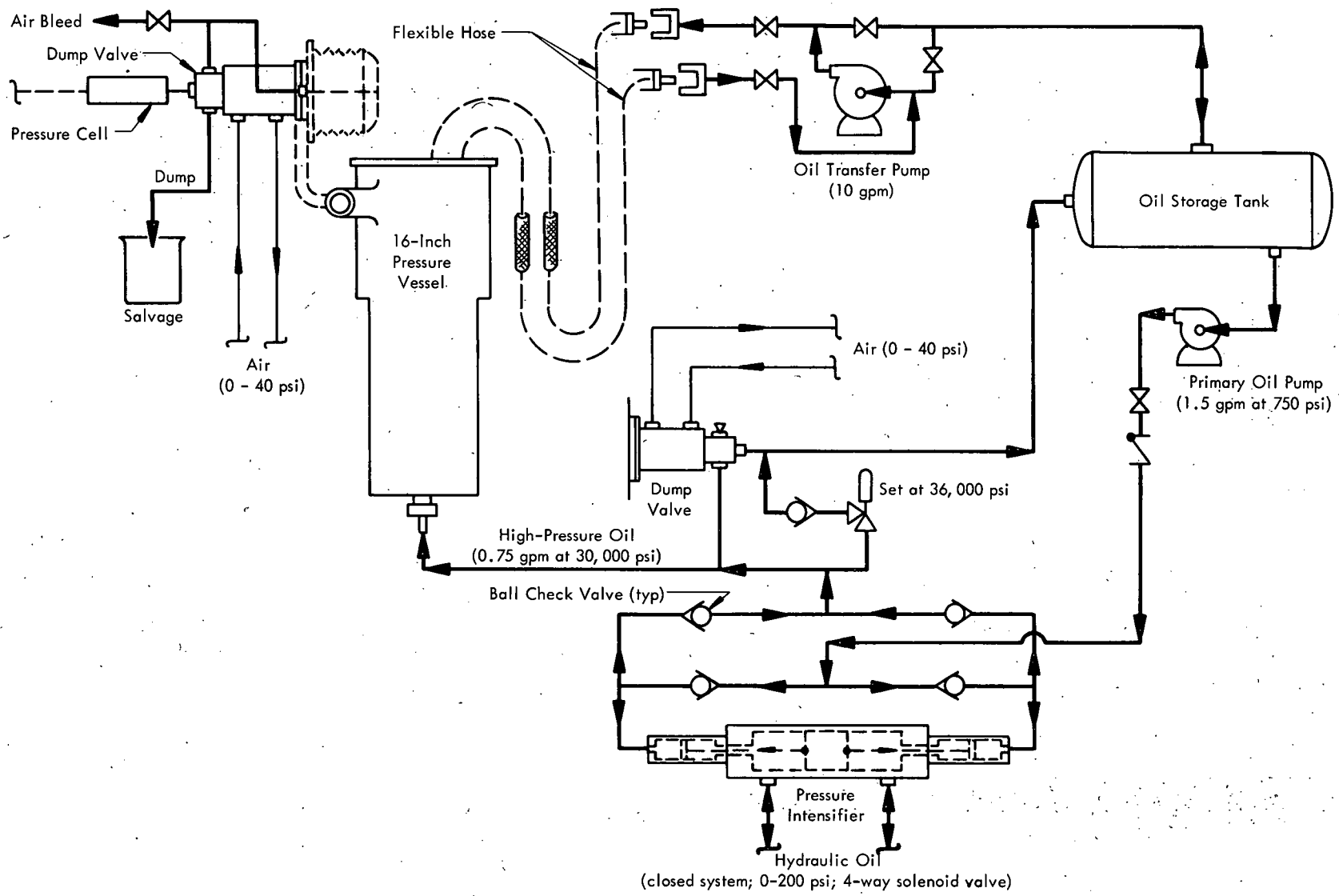

Figure 5. PIPING SYSTEM FOR THE SIXTEEN-INCH PRESSURE VESSEL.

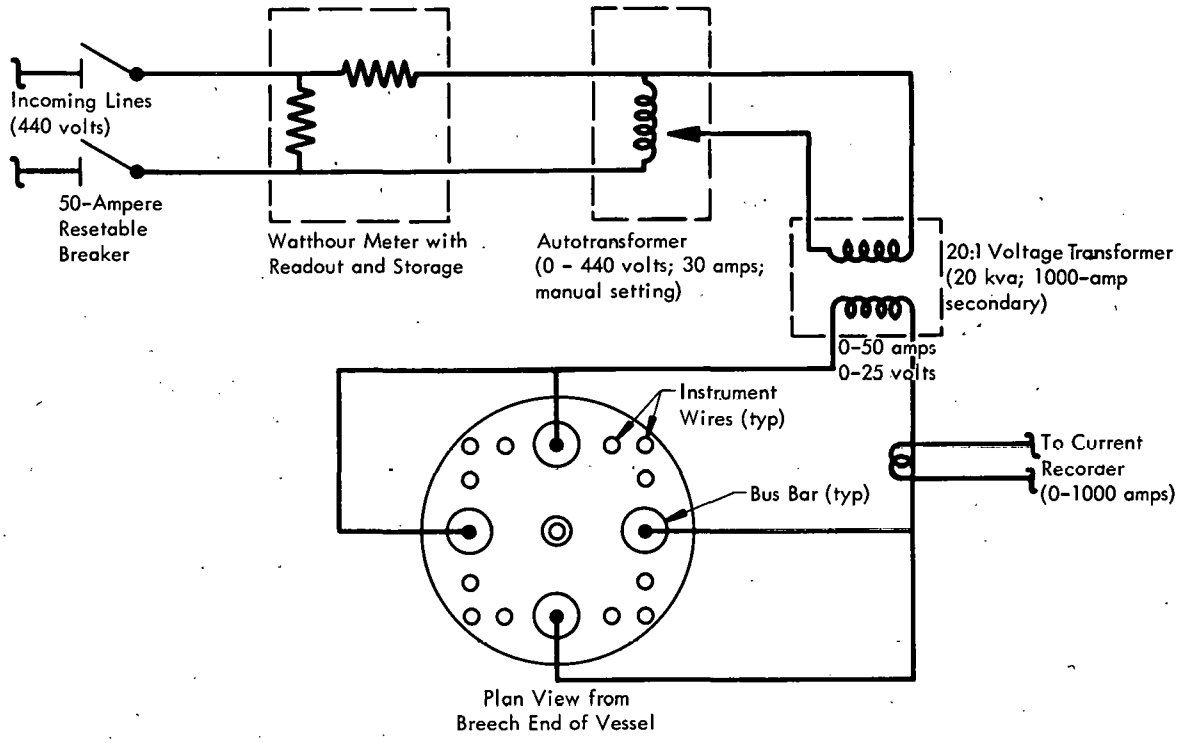

Figure 6. ELECTRICAL SYSTEM FOR THE SIXTEEN-INCH PRESSURE VESSEL.

watt-hour meter equipped with both readout and storage units. The storage unit is used to cut power after a preset heat input. The readout is used for an indication of the amount consumed. The transformed incoming power is fed into 20:1 voltage stepdown transformers rated at 20 kva on the primary and limited to 1000 amperes at the secondary. The load current is recorded at the control panel from an in-line current transformer.

The instrument panel is mounted on a small mobile wagon containing a patch board, the autotransformer, and all recorders. The schematic layout for the instrument panel is given in Figure 7. The recorders are all three-second span electronic machines.(b) The pressure-recording circuit was calibrated against the Aminco dead-weight tester certified to ± 5 psi over the range. The signal reading system resolution is ± 50 psi over the range. The pressure-sensing element is a BLH-SR4 cell. Although the furnace power integral includes the transformer losses, instantaneous power samplings are based on voltage readings obtained at the furnace and recorded on the multirange voltage unit. The panel as shown can be quickly and conveniently plugged up to handle the day-to-day variations needed in any evolutionary operation. Readings obtained on Chromel-Alumel couples are developed through properly compensated leads. Since the platinum-rhodium and tungsten-rhenium readouts are not compensated, the entire loop was calibrated in situ without room-temperature compensation; and the corrections obtained, which were extremely small, were applied during the actual experiments as needed.

(b) Brown Instruments Company.

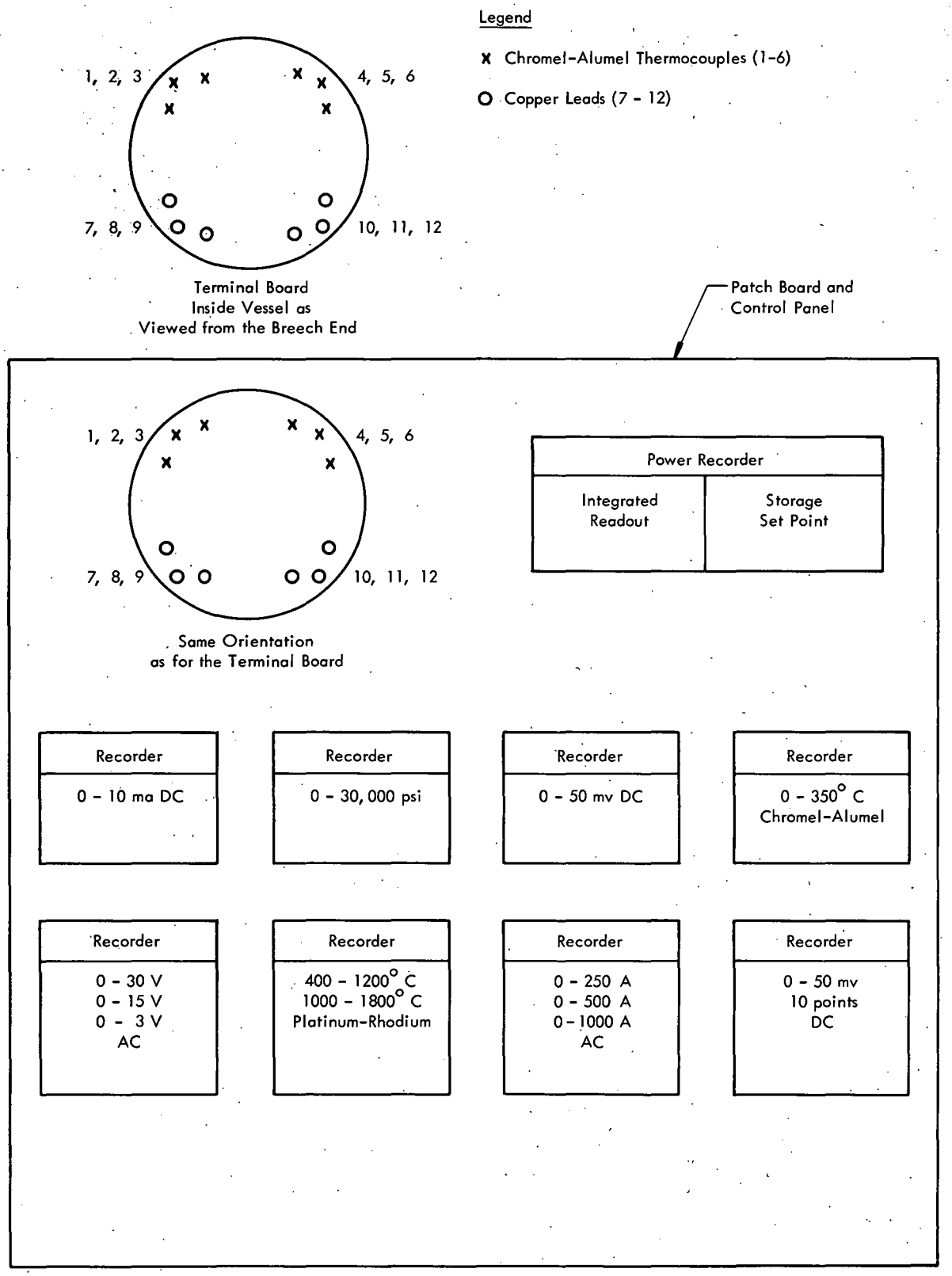

Figure 7. INSTRUMENT SYSTEM FOR THE SIXTEEN-INCH PRESSURE VESSEL.

EXPERIMENTAL PROCEDURE

Pressure Transmission Studies

The entire concept of hot pressing a specimen isostatically in a furnace assembly by hydraulic actuation depends upon obtaining a suitable pressure-transmitting sand. Such a sand must provide adequate insulation, be efficient, give isotropic pressure transmission, and, hopefully, be nonforming; therefore, reusable. The direct measurement of internal sand pressures under the action of oil pressure, although desirable for the evaluation of candidate sands, proved difficult to accomplish on a laboratory scale. An indirect method was employed by forming powder specimens in the candidate sand while it, in turn, was under oil pressure. Uranium dioxide powder has been pressed isostatically over a range of conditions and its forming properties are well known.(9) The general method of measuring the sand pressure then is simply to press a uranium dioxide compact in a mass of candidate sand pressured in turn by oil. The density of the resultant uranium dioxide compact can then be duplicated by direct hydrostatic pressing and the "equivalent" pressure determined.

The uranium dioxide is isostatically formed by first loosely filling a latex bag with the powder. The bag has a thickness of four to six mils, is six inches long, and is held in a fixture (Figure 8). The bag is stretched and held in place by evacuating the fixture (Step 1). After filling to the desired depth, a porous cardboard disc is dropped on the powder surface to provide a square corner after pressing, as shown in Step 1. The bag is then rolled back off the fixture onto a second tube so that the powder compact is brought under vacuum (Step 2). After compact evacuation, air is admitted to the fixture to release the compact. A simple knot in the latex seals the compact (Step 3). The compact at this point is 1/2 inch in diameter and one inch long (Step 4). It is immersed in oil and pressed.

The physical properties of the chosen uranium dioxide are given in Table 1. The pressure-density relation is plotted over the range to 650,000 psi in Figure 9. As indicated, the density change per unit pressure change is large, thus providing good pressure resolution. The lower pressure portion of the curve is of particular interest and is shown enlarged in Figure 10. Two further properties of the cold-pressed uranium dioxide compacts must be evaluated prior to its use for sand-pressure calibration. Referring to Figure 9, the circled numbers show there is a persistent gain in compact density as it is successively repressed at a given pressure. The repress pressure indicated was 50,000 psi. The data are plotted in more detail in Figure 11. Ideally, the diametral shrinkage should be just half the longitudinal. Since this is not quite the case, there appears to be some preferential shrinkage during isostatic pressing. This factor must be considered in evaluating the "isostaticity" of candidate sands.

The sand pressure transmission tests were carried out in the apparatus shown in Figure 12. The pellets, prepared as described in Figure 8, were buried in a test sand in a larger but similarly evacuated latex bag which was about 5/8 inch in diameter and

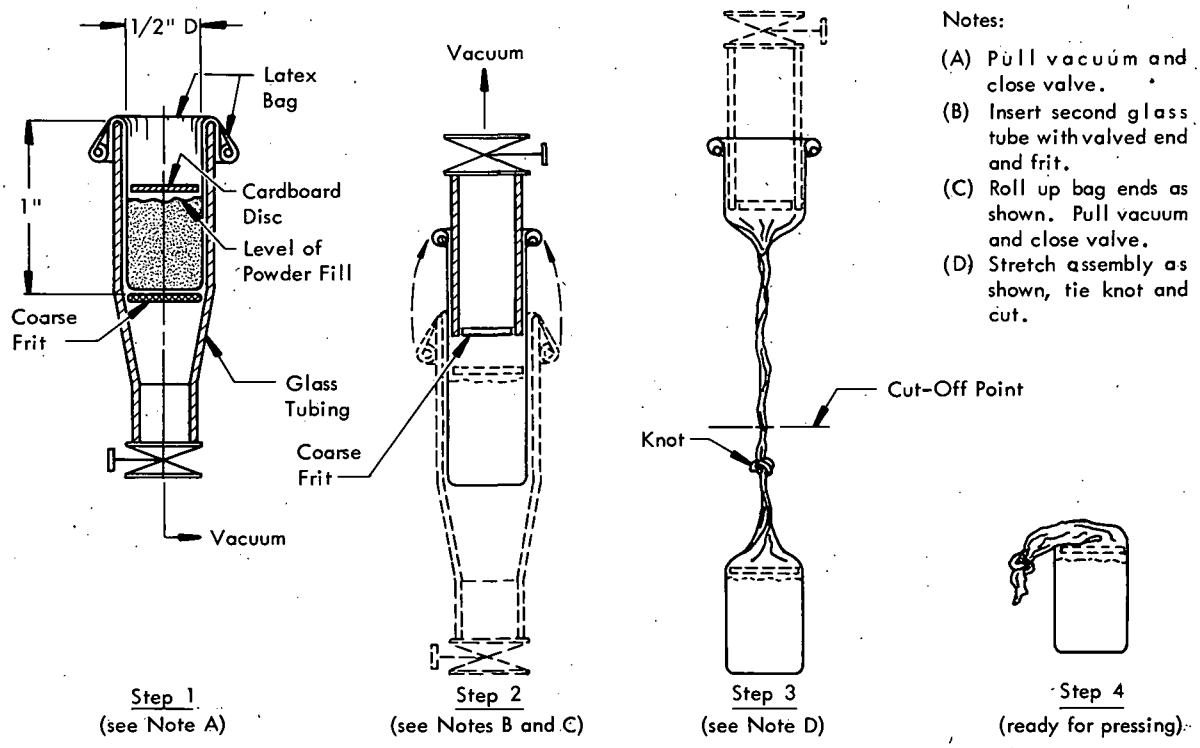

Figure 8. FORMING FIXTURE FOR THE EXPERIMENTAL POWDER PRESSING EXPERIMENT.

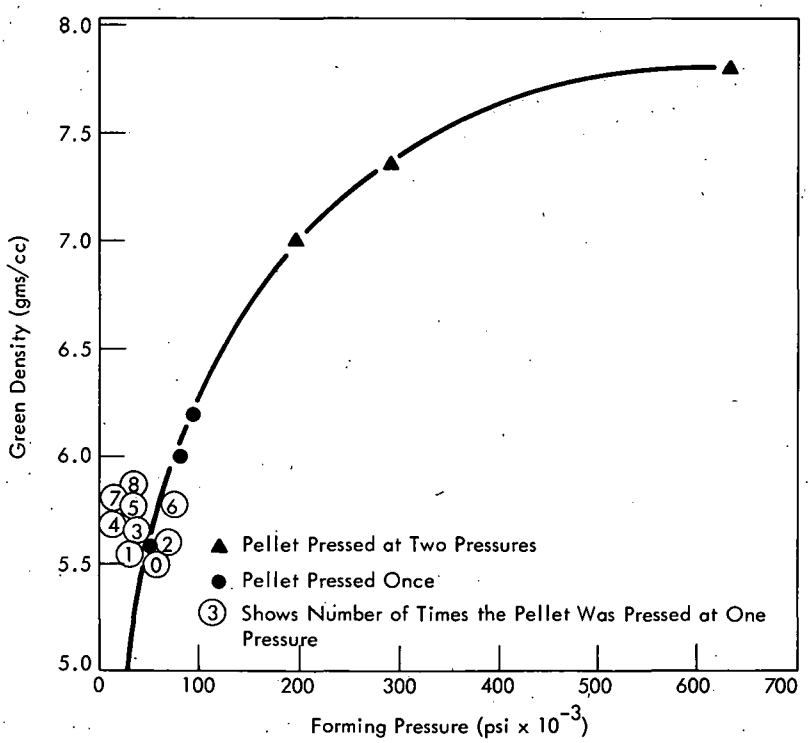

Figure 9. DENSITY OF SINTERABLE URANIUM DIOXIDE POWDER AS A FUNCTION OF THE ISOSTATIC FORMING PRESSURE. (From 0 to 650,000 psi)

Table 1

PHYSICAL PROPERTIES OF SINTERABLE URANIUM DIOXIDE USED IN SAND PRESSURE STUDIES

Grams U/gram Dioxide	0.86747
Grams U^{+6}/gram Dioxide	0.1635
Surface Area	5.42 m^2/gm
Mesh Size	All -200 mesh
Agglomerate Size (Sharple's Micromerograph)	10% < 1 μ, 50% < 4 μ, 90% < 15 μ
Major Impurities	W < 100 ppm, Fe < 65 ppm
O:U Ratio	2.14:1

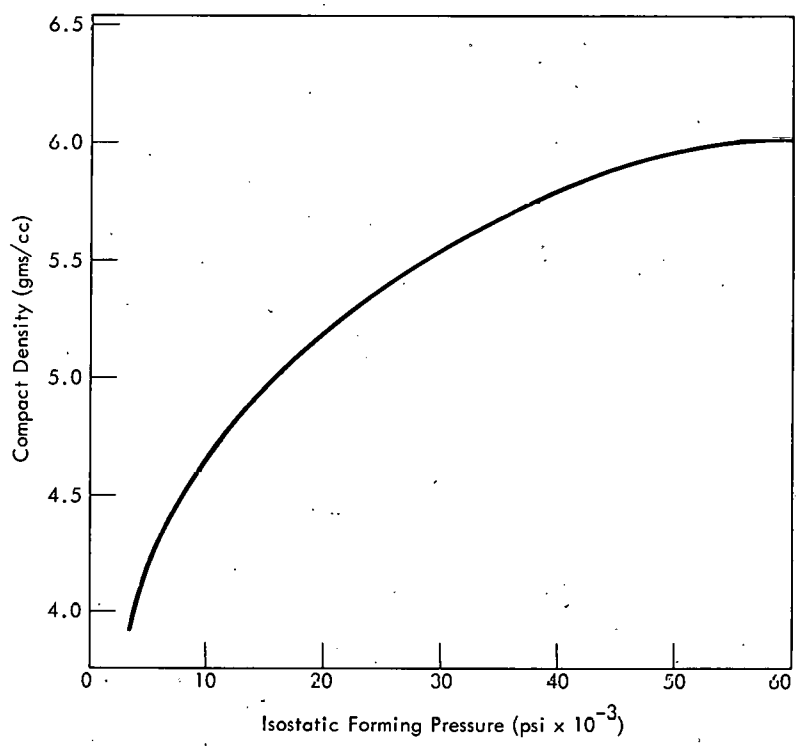

Figure 10. DENSITY OF SINTERABLE URANIUM DIOXIDE POWDER AS A FUNCTION OF THE ISOSTATIC FORMING PRESSURE. (From 0 60,000 psi)

1 1/2 inches long. The assembly was dropped into oil in a pressure vessel for pressing. The vessel pistons were actuated in a conventional 200-ton press that was independently calibrated. The first sand media chosen for the test were as listed in Table 2.

These materials were chosen because they were found to be nonforming at 50,000 psi and because of the wide range in Poisson's ratio provided. Test assemblies, such

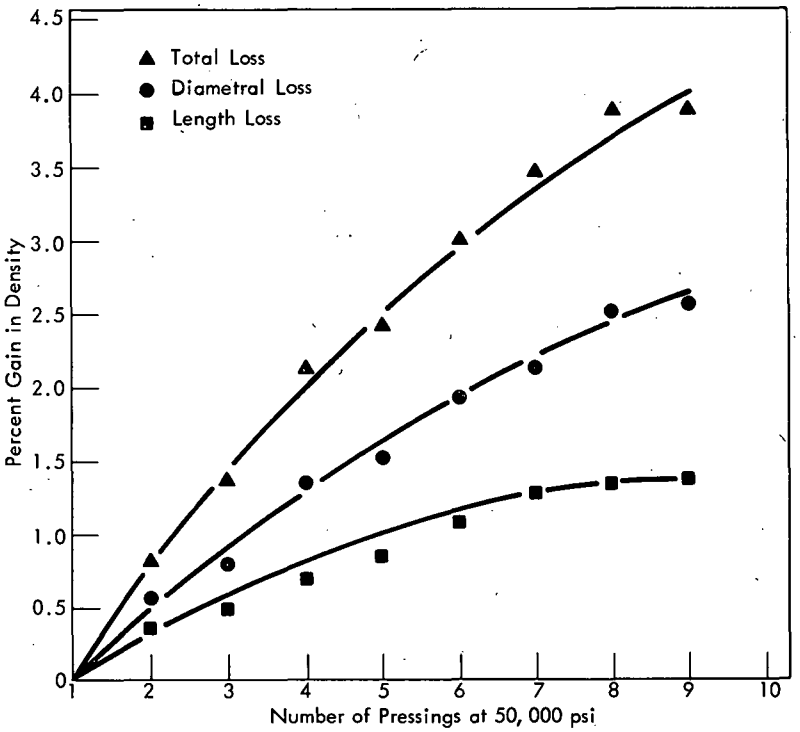

Figure 11. PERCENT DENSITY GAIN IN URANIUM DIOXIDE COMPACTS AS A FUNCTION OF THE INDEPENDENT ISOSTATIC REPRESSINGS AT 50,000 PSI.

Table 2

SAND MEDIA USED IN TEST PRESSINGS

Sand	Mesh	Poisson's Ratio
SiC	600	0.12
Al_2O_3	200	0.22
Cr_2O_3	100	0.30

as shown in Figure 12, were pressed at 50,000 psi four times. Results are summarized in Figure 13. The density change was more rapid in all sands than in oil alone. The density increase ranged from 4 to 6% in the various sands and was but 2 1/4% in oil alone. The increase was greatest in alumina; least in silicon carbide. The results are brought out in detail in Figures 14 through 16. As in the case with direct oil pressing, the diametral shrinkage lags the longitudinal and the density gains over direct pressing are real. Since the gain appeared most pronounced in the alumina sand, several experiments were made at a pressure of 30,000 psi. Of course, the eventual application of sand transmission on a large scale would be utilized at 30,000 psi or less because this is the ceiling pressure of the large vessels. However, a pressure of 50,000 psi was used at this point to magnify the density gain, if any, observed. Results of the 30,000-psi experiments are summarized in Figure 17. After five repressings, the density increase of sand results over oil were consistently higher

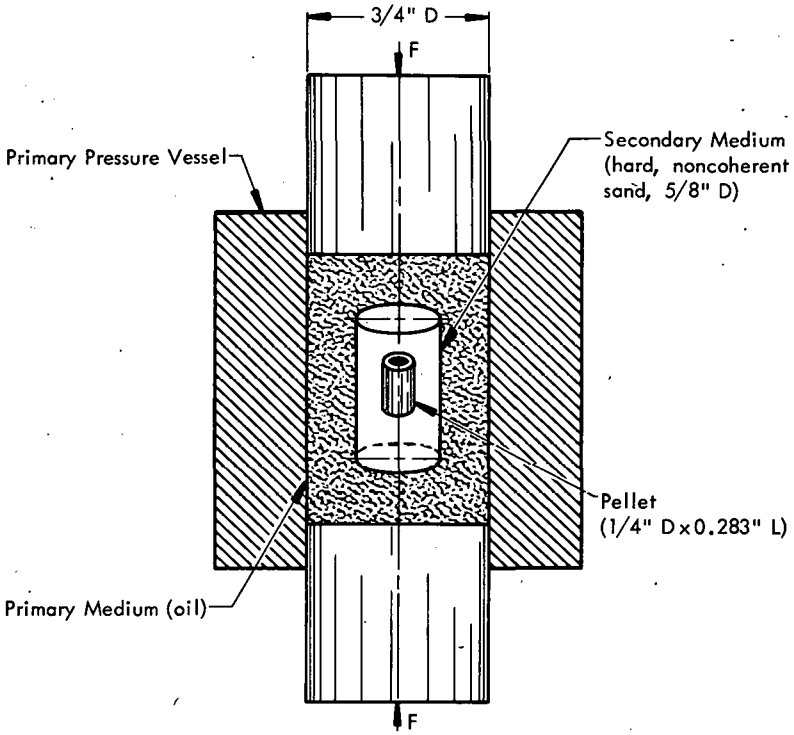

Figure 12. EXPERIMENTAL SAND PRESSURE-TRANSMISSION TEST SETUP.

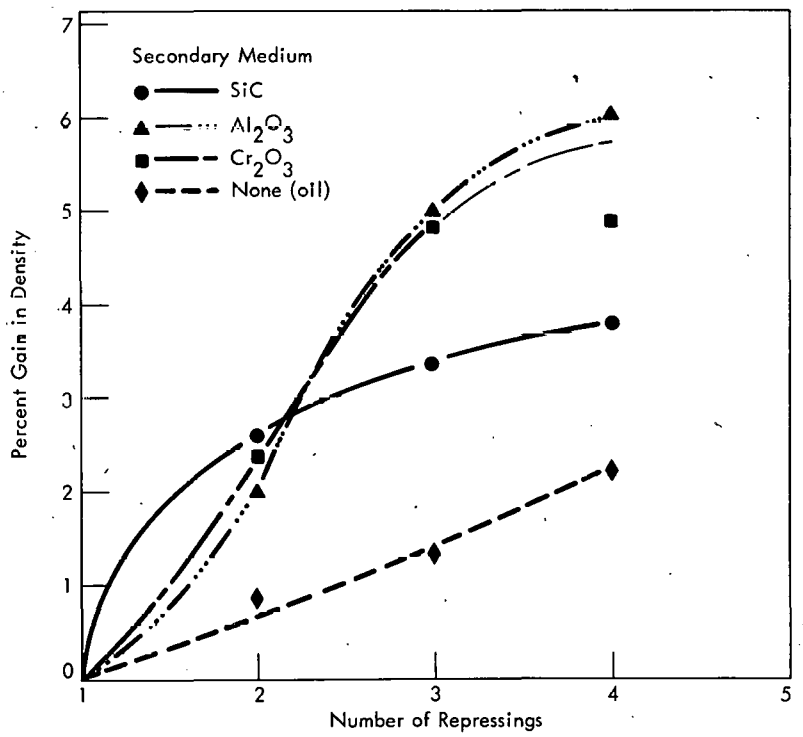

Figure 13. PERCENT INCREASE IN THE URANIUM DIOXIDE COMPACT DENSITY AS A FUNCTION OF THE NUMBER OF REPRESSINGS AT 50,000 PSI IN VARIOUS SAND MEDIA – ACTUATED BY OIL.

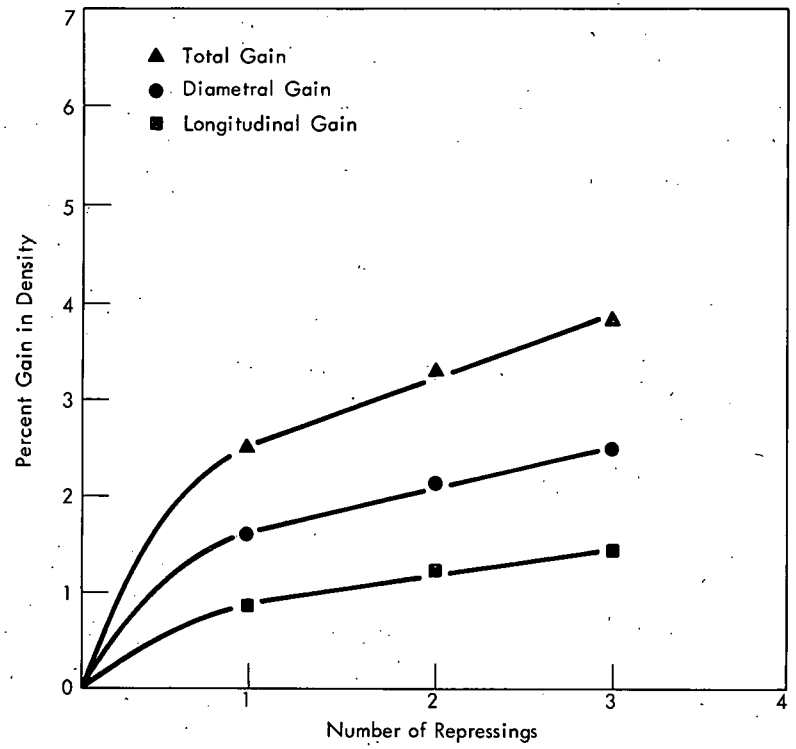

Figure 14. PERCENT INCREASE IN THE URANIUM DIOXIDE COMPACT DENSITY AS A FUNCTION OF THE NUMBER OF REPRESSINGS AT 50,000 PSI IN A SILICON CARBIDE SAND MEDIUM – ACTUATED BY OIL.

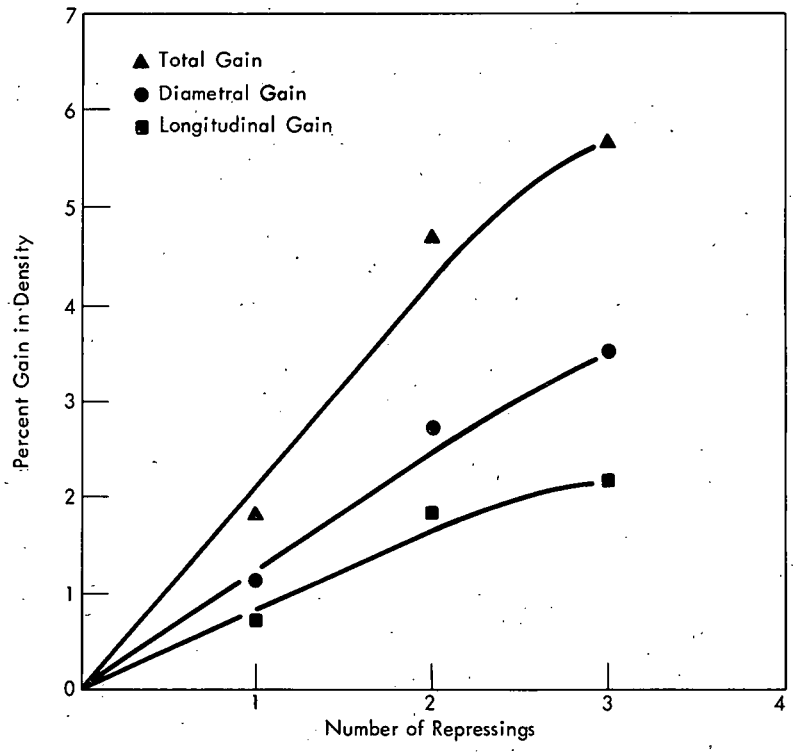

Figure 15. PERCENT INCREASE IN THE URANIUM DIOXIDE COMPACT DENSITY AS A FUNCTION OF THE NUMBER OF REPRESSINGS AT 50,000 PSI IN AN ALUMINA SAND MEDIUM – ACTUATED BY OIL.

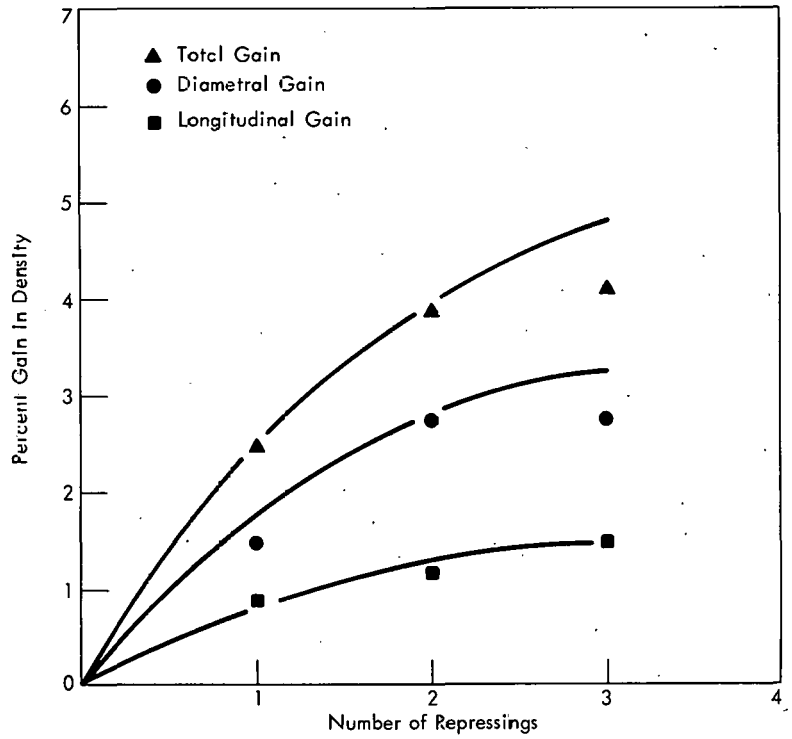

Figure 16. PERCENT INCREASE IN THE URANIUM DIOXIDE COMPACT DENSITY AS A FUNCTION OF THE NUMBER OF REPRESSINGS AT 50,000 PSI IN A CHROMINA SAND MEDIUM – ACTUATED BY OIL.

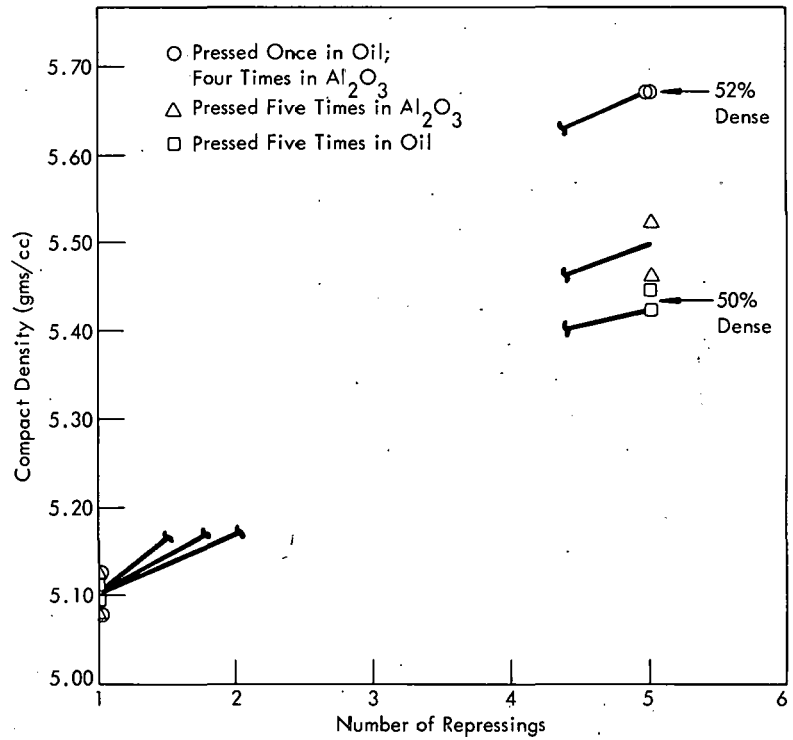

Figure 17. URANIUM DIOXIDE DENSITY WHEN THE POWDER IS PRESSED IN ALUMINA SAND AS A FUNCTION OF THE NUMBER OF REPRESSINGS AT 30,000 PSI – ACTUATED BY OIL.

but the difference was not statistically significant. When pressed first in oil and repressed in sand, a significant density difference after five represses was found.

Although the density gain at 30,000 psi in a single press was less than statistically significant in the experiments previously described, there was never any suggestion of a pressure loss in transmission either radially or longitudinally. A second series of sand-transmission studies were made on a larger scale. A polyvinyl bag was obtained which had inside dimensions of 13 inches in diameter and 13 inches long. The bag was filled with test sands of magnesia, alumina, and natural flake graphite. The initial pellets were formed in the usual way at 800 psi and positioned in the sand, as shown in Figure 18, with three pellets of each sand merely immersed in the actuating oil. Results obtained with the various media are summarized in Tables 3 through 5. As indicated, the individual pellet densities after very-low-pressure isostatic forming and after the single sand repress show no statistically significant density changes.

The question of pressure transmission in a spherical geometry was investigated using a 12-inch-ID rubber sphere. The sphere was filled with alumina sand with the

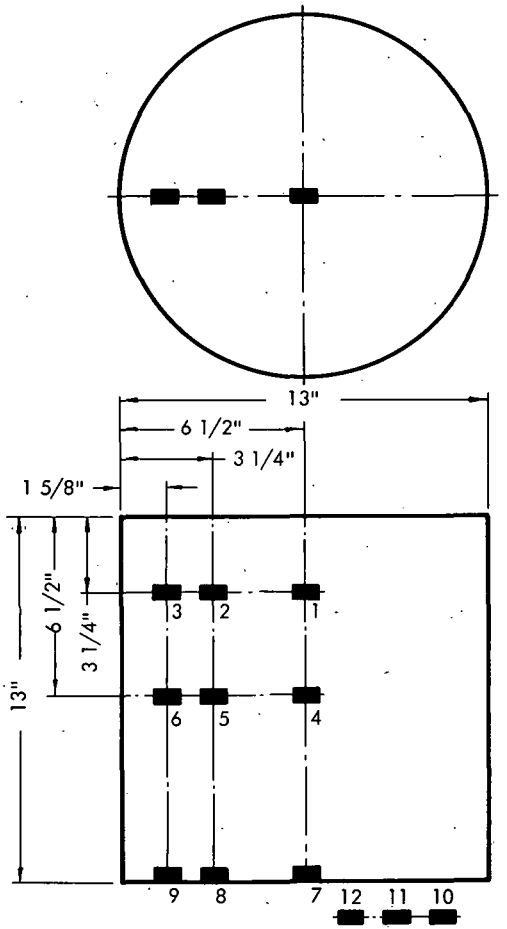

Figure 18. LARGE-SCALE SAND PRESSURE-TRANSMISSION TEST. (Pellet Location)

Table 3

URANIUM DIOXIDE DENSITY CHANGE AFTER PRESSING IN FOUR TO EIGHT-MESH MAGNESIA SAND AT 30,000 PSI

Pellet Number(1)	Secondary Medium	Average Density(2) Pressed in Oil (gms/cc)	Average Density(2) Pressed in Magnesia (gms/cc)	Increase in Density (%)
1	MgO	4.96	4.99	+0.6
2	MgO	4.96	4.87	-1.8
3	MgO	4.96	4.97	+0.2
4	MgO	4.96	4.96	0.0
5	MgO	4.96	4.98	+0.4
6	MgO	4.96	4.95	-0.2
7	MgO	4.96	4.95	-0.2
8	MgO	4.96	4.97	+0.2
9	MgO	4.96	4.92	-0.8
10	Oil	4.96	4.93	-0.6
11	Oil	4.96	4.99	+0.6
12	Oil	4.96	4.97	+0.2

(1) Pellets prepressed at 800 psi.
(2) Pellets pressed at 22,500 psi.

Table 4

URANIUM DIOXIDE DENSITY CHANGE AFTER PRESSING IN FORTY-MESH ALUMINA AT 30,000 PSI

Pellet Number(1)	Secondary Medium	Average Density(2) Pressed in Oil (gms/cc)	Average Density(2) Pressed in Magnesia (gms/cc)	Increase in Density (%)
1	Al_2O_3	5.44	5.45	+0.2
2	Al_2O_3	5.44	5.45	+0.2
3	Al_2O_3	5.44	5.41	-0.6
4	Al_2O_3	5.44	5.37	-1.3
5	Al_2O_3	5.44	5.38	-1.1
6	Al_2O_3	5.44	5.44	0.0
7	Al_2O_3	5.44	5.37	-1.3
8	Al_2O_3	5.44	5.44	0.0
9	Al_2O_3	5.44	5.42	-0.4
10	Oil	5.44	5.42	-0.4
11	Oil	5.44	5.43	-0.2
12	Oil	5.44	5.48	+0.9

(1) Pellet prepressed at 800 psi.
(2) Pellet pressed at 30,000 psi.

uranium dioxide pellets located as shown in Figure 19. The pellets were first pressed in oil at 30,000 psi and then repressed in the sand at 30,000 psi, with the results given in Table 6. In this arrangement, a distinct loss in transmission was noted; therefore, experiments in spheres were abandoned.

A final pellet-pressing experiment in a 200-mesh alumina medium and the cylindrical geometry of Figure 18 was undertaken in which the pellets were first formed isostatically at 22,500 psi and repressed in the sand seven times at 30,000 psi. The results of this experiment are reported in Table 7. As can be seen, the sand-pressed densities are consistently low and the difference is not statistically significant.

Table 5

URANIUM DIOXIDE DENSITY CHANGE AFTER PRESSING IN NATURAL FLAKE GRAPHITE AT 30,000 PSI

Pellet Number(1)	Secondary Medium	Average Density(2) Pressed in Oil (gms/cc)	Average Density(2) Pressed in Graphite (gms/cc)	Increase in Density (%)
1	NFG	5.46	5.38	-1.5
2	NFG	5.46	5.31	-2.7
3	NFG	5.46	5.32	-2.7
4	NFG	5.46	5.31	-2.7
5	NFG	5.46	5.29	-3.1
6	NFG	5.46	5.22	-4.4
7	NFG	5.46	5.29	-3.1
8	NFG	5.46	5.25	-3.8
9	NFG	5.46	5.22	-4.4
10	0.1	5.46	5.49	+0.5
11	0.1	5.46	5.46	0.0
12	0.1	5.46	5.44	-0.4

(1) Pellets prepressed at 800 psi.
(2) Pellets pressed at 30,000 psi.

Table 6

URANIUM DIOXIDE DENSITY CHANGE AFTER PRESSING IN 200-MESH ALUMINA IN A SPHERICAL GEOMETRY AT 30,000 PSI

Pellet Number(1)	Secondary Medium	Average Density(2) Pressed in Oil (gms/cc)	Average Density(2) Pressed in Alumina (gms/cc)	Increase in Density (%)
1	Al_2O_3	5.40	5.22	-3.3
2	Al_2O_3	5.40	5.24	-3.0
3	Al_2O_3	5.40	-	-
4	Al_2O_3	5.40	5.28	-2.2
5	Al_2O_3	5.40	5.28	-2.2
6	Al_2O_3	5.40	5.26	-2.6
7	Oil	5.40	5.39	-0.2
8	Oil	5.40	5.41	+0.2

(1) Pellets prepressed at 800 psi.
(2) Pellets pressed at 30,000 psi.

The 13-inch cylindrical plastic bag was fitted with a lid (separately described; Page 29) containing a pair of Size 16 copper wire leads. Two matched noninductively wound manganin coils were obtained that had a resistance of 120 ± 0.1 ohms and were 1/8 inch in diameter and 1/2 inch long. When immersed in a hydrostatic pressure field, the coils have a resistance response of 1.6×10^{-7} ohms/ohm/psi. One coil was immersed and sealed in a small glycerine-filled bag that was 1/4 inch in diameter and 1 inch long. This assembly was buried in four to eight-mesh magnesia sand along the 13-inch-diameter bag centerline about seven inches deep. The 13-inch-D bag was immersed in the vessel with the second manganin coil immersed in gun oil. Coil readouts were read on the same bridge through identical wiring. The vessel was put under 15,000-psi pressure. The results of the sand pressure-oil pressure responses are plotted in Figure 20.

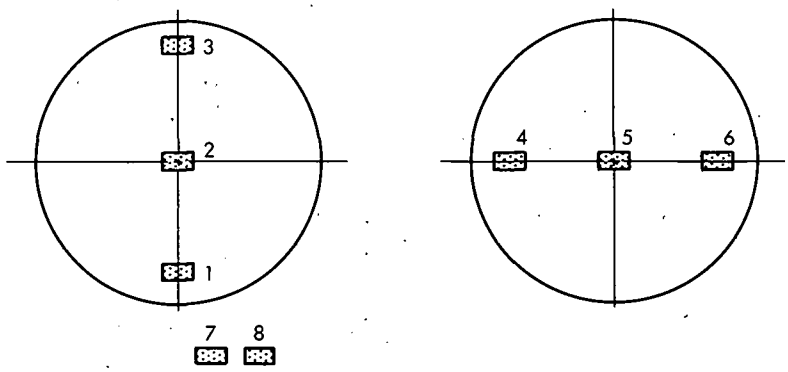

Figure 19. ARRANGEMENT OF SPECIMENS IN THE SPHERICAL SAND PRESSURE-TRANSMISSION TEST.

Table 7

URANIUM DIOXIDE DENSITY CHANGE AFTER SEVEN REPRESSINGS IN 200-MESH ALUMINA SAND IN A CYLINDRICAL GEOMETRY AT 30,000 PSI

Pellet Number(1)	Secondary Medium	Average Density(2) Pressed in Oil (gms/cc)	Repressed in Oil (gms/cc)	Repressed in Alumina (gms/cc)	Increase in Density(3) (%)
1	Oil	4.88	5.48	-	12.3
2	Oil	4.88	5.45	-	11.7
3	Oil	4.88	5.48	-	12.3
4	Al_2O_3	4.88	-	5.40	10.7
5	Al_2O_3	4.88	-	5.40	10.7
6	Al_2O_3	4.88	-	5.40	10.7
7	Al_2O_3	4.88	-	5.33	9.2
8	Al_2O_3	4.88	-	5.36	9.8
9	Al_2O_3	4.88	-	5.37	10.0
10	Al_2O_3	4.88		5.35	9.6
11	Al_2O_3	4.88	-	5.35	9.6
12	Al_2O_3	4.88	-	5.34	9.4

(1) Pellets prepressed at 800 psi.
(2) Pellets pressed at 22,500 psi in oil and at 30,000 psi in the alumina.
(3) Average alumina pressed density increase - 10.0%; average oil pressed density increase - 12.1%.

As indicated, the pressures rise together smoothly. However, during the pressure relief (fall), the sand "holds back" such that the specimen pressure is about 3000 psi greater than the hydraulic during most of the decay. The final pressures agree closely.

Operational Bag Evaluation

One phase of the study called for immersing a specimen-furnace assembly in an insulating, pressure-transmitting sand. To accomplish this it was necessary to contain the sand in some way so that an oil seal could be provided and still meet the requirement of high compliance for good pressure transmission and sufficient ductility to provide for sand shrinkage. To this end, a polyvinyl chloride chamber was constructed, shown schematically in Figure 21. This bag and seal design, including the

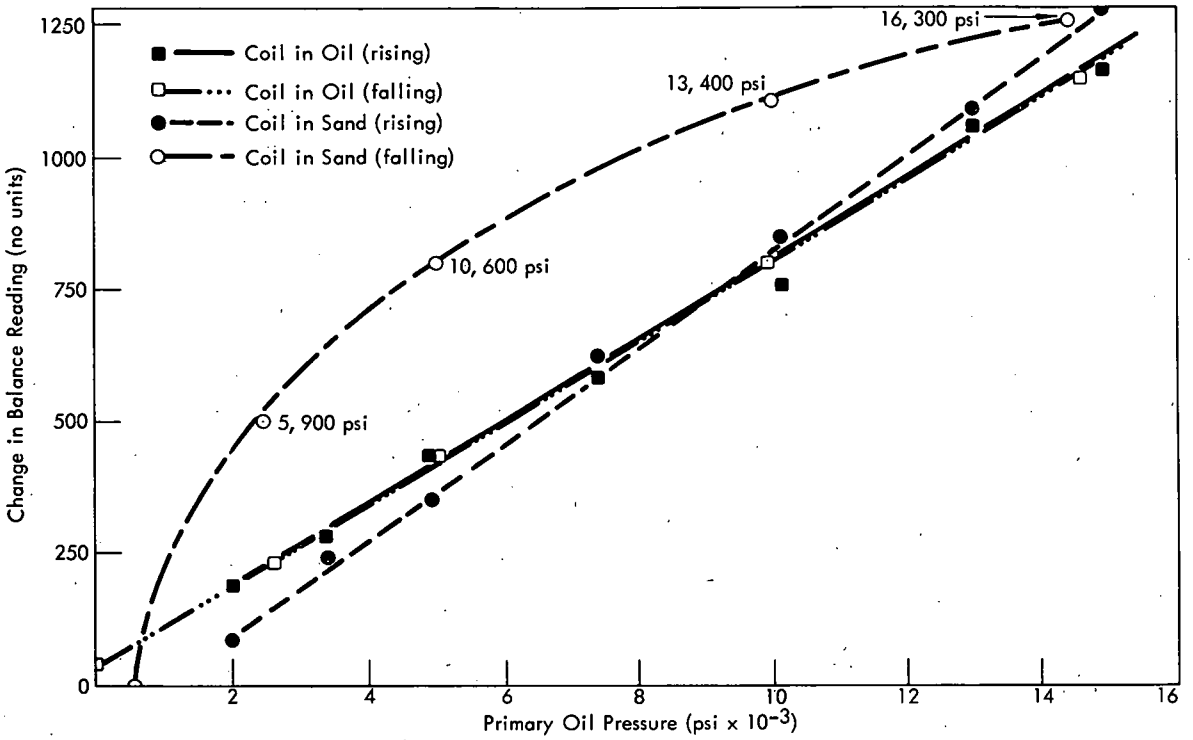

Figure 20. COIL RESPONSE IN FOUR TO EIGHT-MESH MAGNESIA SAND AND IN OIL AS FUNCTIONS OF THE PRIMARY (VESSEL) OIL PRESSURE.

evacuation port, had been in regular use in cold-pressing operations. Tests with cold pressings in 4 to 200-mesh magnesia proved that the seal was dependable and the bag reusable.

A second requirement basic to the sand-pressing project was adequate electrical communication. This need was successfully met by casting a pair of 3/4-inch-diameter copper bus bars and eight Size 14 instrument leads into the lid. The location of these leads is indicated in Figure 22. The copper bus bar was machined from barstock with the disc protrusions slightly thicker at the edge than at the column blend. The discs were grooved bars to enhance the bond. The lead ins and bus bars were coated with plastic prior to casting the lid. The lid mold provided positive placement for the lead ins. A more detailed elevation of the mold and lid is shown in Figure 23. The bags and lids were all made of polyvinyl chloride. The polyvinyl plastisol was poured into the mold and cured in air at 160 to 180° C to produce the part.

Nonpressurized Furnace Experiments

The furnace characteristics of an actual bag assembly were examined prior to the pressure test. The test arrangement is shown in section in Figure 24. The specimen was a cold-pressed bar of tungsten and alloying powders that was two inches in diameter and six inches long. The coil was made from two molybdenum strips layed back

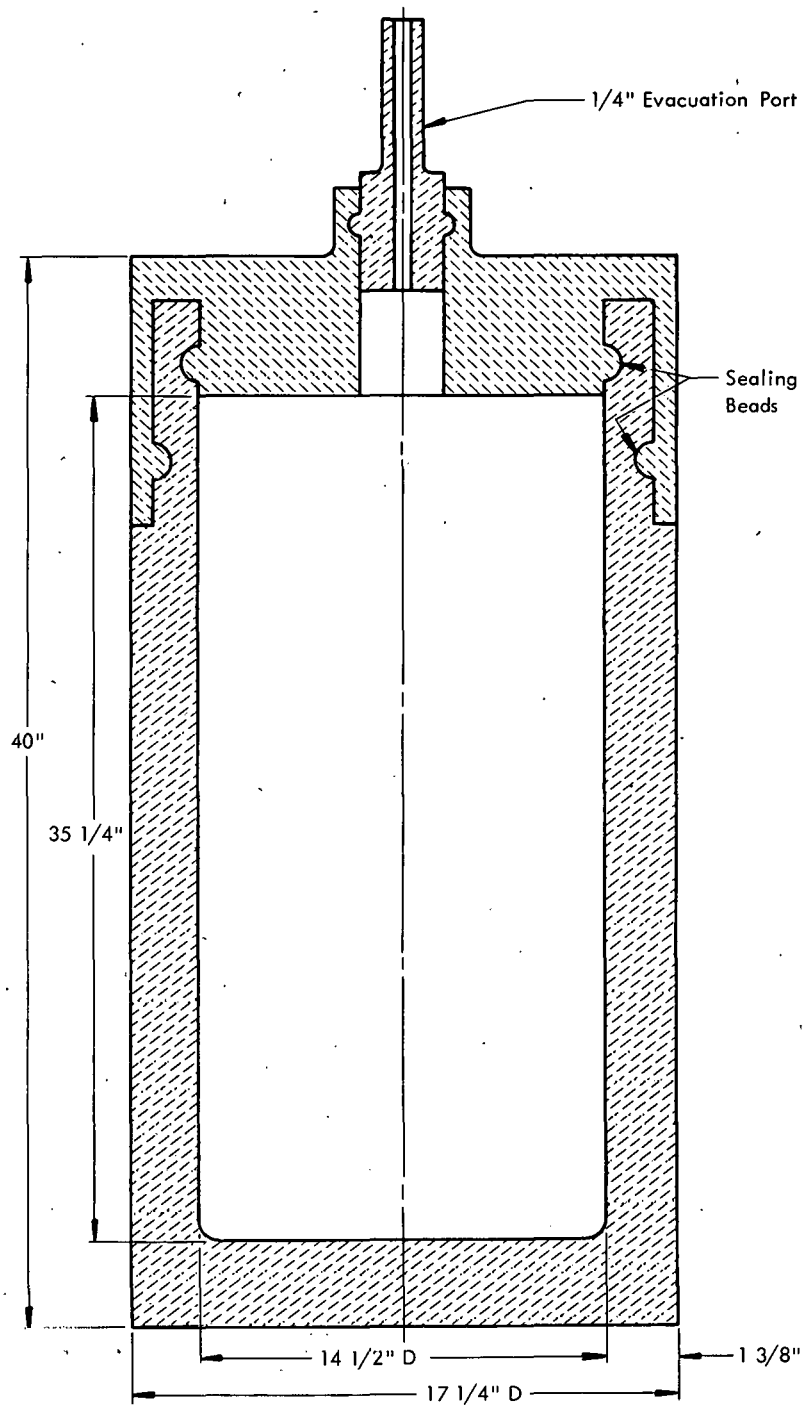

Figure 21. POLYVINYL CHLORIDE SAND-CONTAINMENT BAG.

to back. Each strip was 1/2 inch wide, 0.020 inch thick, and 72 inches long. The coil was formed in herpetic fashion on a mandrel using a welding torch to bend the strip. The last six inches of the strips were overlaid with additional strips and wire wound to provide cool terminals. The finished coil was about three inches in diam-

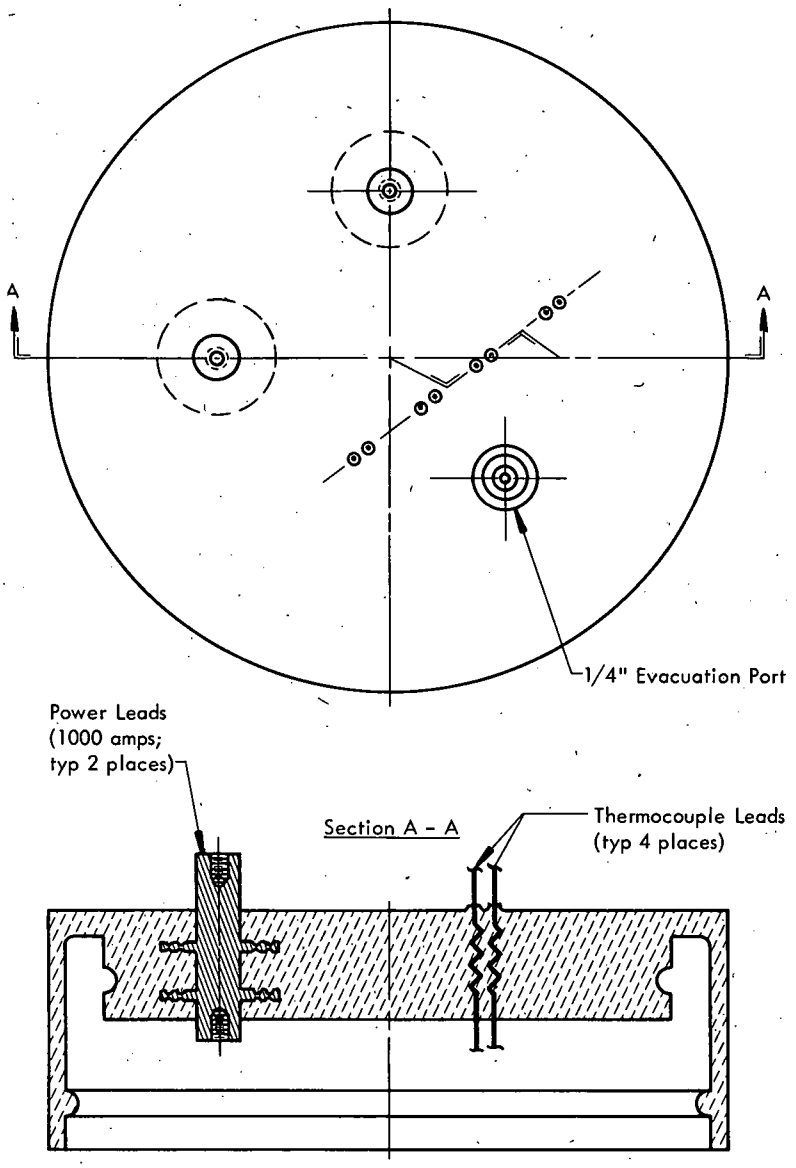

Figure 22. ELECTRICAL LEADS THROUGH THE LID INTO THE POLYVINYL CHLORIDE BAG.

eter and 12 inches long. Welding cable was used at the juncture. The assembly (Figure 24) was built up by filling with sand to a given depth, setting in the coil, continuing the fill a bit, setting in the specimen, continuing the fill, then adding more sand. Thermocouples were also located as shown. The juncture at the lid inside is accomplished with ordinary line connectors for thermocouple leads. The power leads are bolted to the bus bars. After setting the leads, the lid beads (Figures 21 and 22) were lubricated with stopcock grease and the lid pressed in place. The bag was evacuated.

After evacuation, one kilowatt of power was applied which brought the part to 1000° C in 20 minutes. The holding power was 0.56 kilowatt. After four hours a temper-

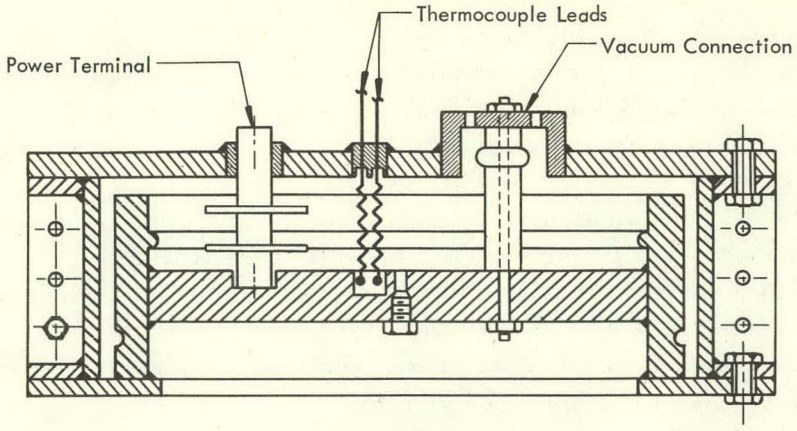

Figure 23. LID-MOLD TOP ASSEMBLY.

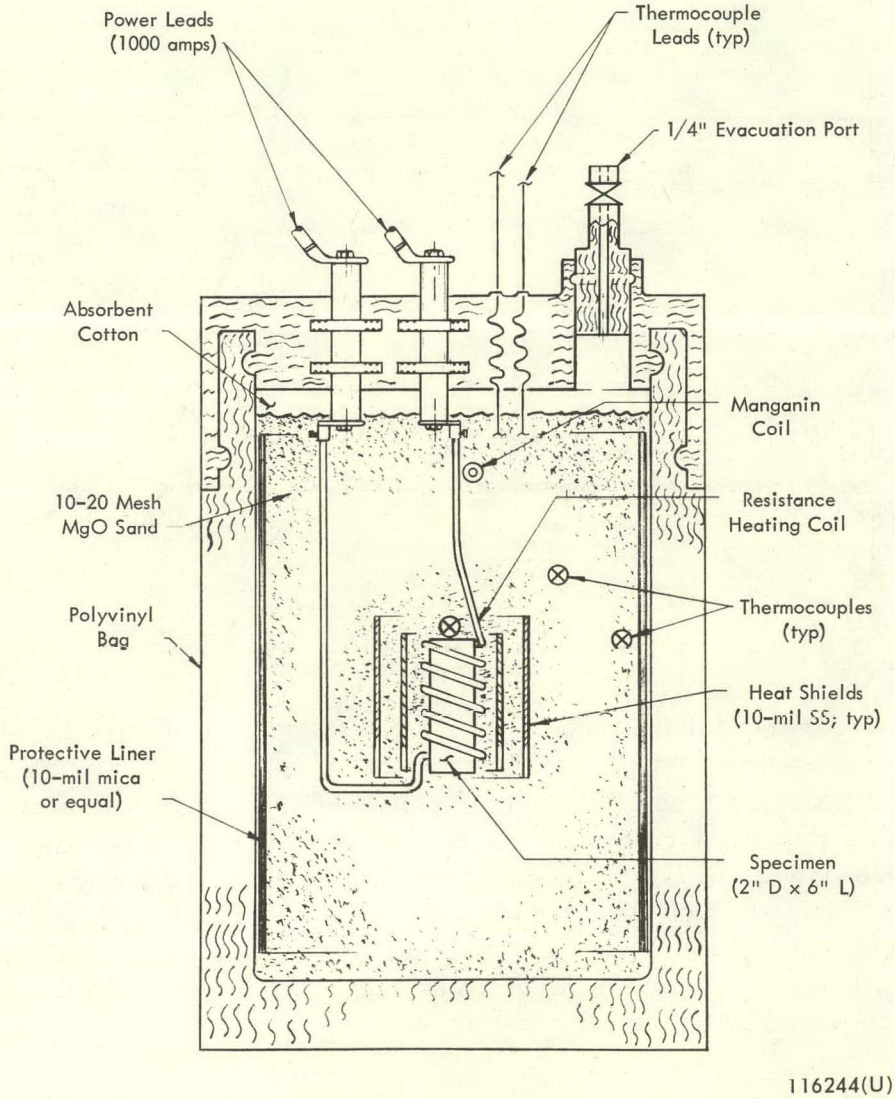

Figure 24. COMPLETE BAG ASSEMBLY FOR THE HOT-PRESS EXPERIMENT.

ature wave was observed at the bag inner skin. These data are summarized by the graph in Figure 25. During this period the system was pumped. Some outgassing was observed for a period but a residual pressure under 1 mm Hg was finally obtained. Referring to Figure 25, note that although the specimen was readily heated and the holding power was very low, there was a delayed but substantial increase in the temperature of the inner surface of the containing bag. The time required to reach a peak temperature at the skin was sufficient to assume that this temperature was simply related to the total heat input. Results from two additional laboratory runs made at an input rate of 1.5 kilowatts are plotted in Figure 26. The specimen heating curve as a function of input power and the subsequent cooling curves for these two tests are given in Figures 27 and 28.

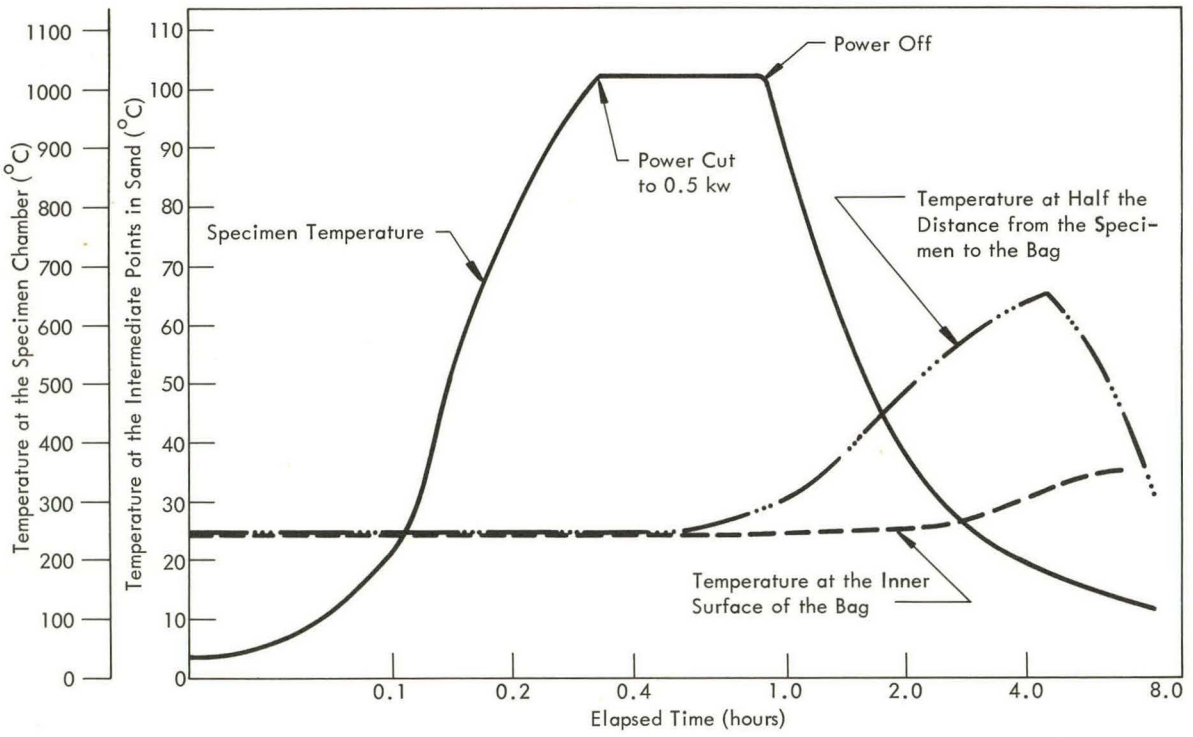

Figure 25. TEMPERATURE RESPONSE OF THE BAG ASSEMBLY WITHOUT PRESSURE.

For hot-press studies, the bag was inverted and set on a stand at a convenient height in the pressure vessel. A cutaway view of the bag in the vessel is shown in Figure 29. The inversion serves two purposes: (1) a more direct connection is made to the heavy cable coming up from the bottom (the cable does not require annular clearance), and (2) the bottom sits on a heavy fixture and this, in common with natural convection, keeps the heat-sensitive feedthroughs cool. Inversion of the bag is accomplished with a suitably designed fixture.

The heat cycle was begun prior to immersing the bag in the vessel because an increase in pressure causes a loss in the insulating value of the sand. This fact was

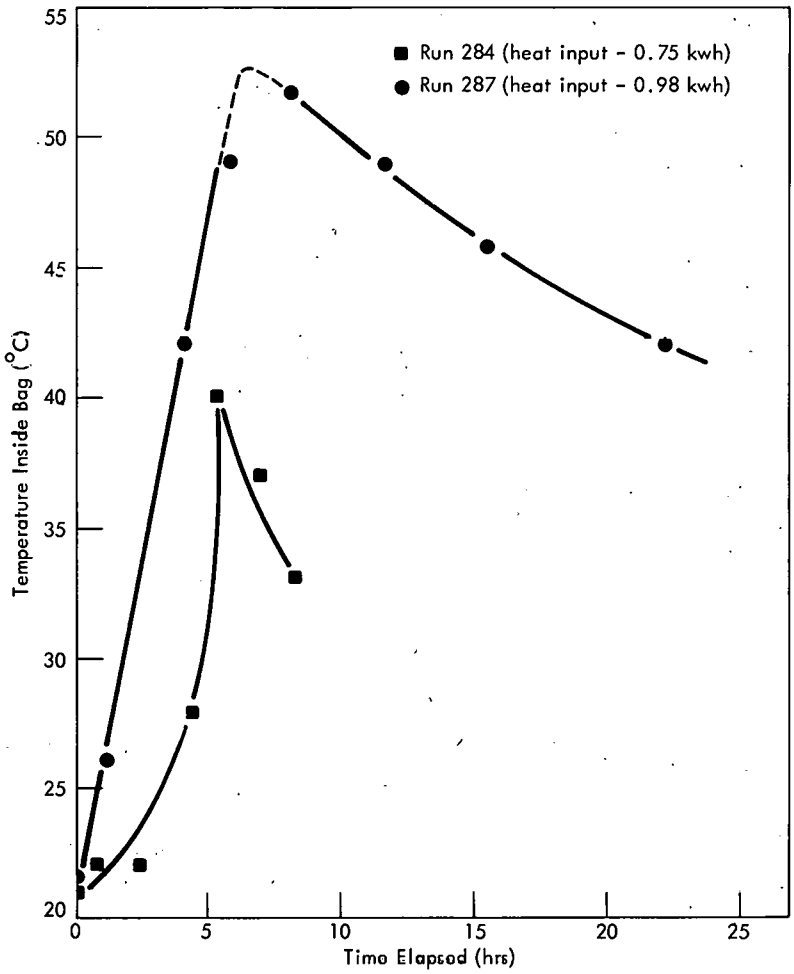

Figure 26. INNER BAG SURFACE TEMPERATURE AS A FUNCTION OF THE ELAPSED TIME FOR TWO HEAT INPUTS. (Power Level – 1.5 Kilowatts)

immediately apparent in the falling temperature at the specimen. Typical specimen heating curves as a function of the heat input are shown in Figure 30. Figure 31 shows the specimen cooling curves. The inner bag surface temperature-time relationship is shown in Figure 32. Higher sand conductivity and a greatly increased operating power requirement under pressure dramatically increased the bag wall temperature excursion. This situation is illustrated in Figure 32. The maximum bag skin temperature, as a function of the input power, is plotted in Figure 33. Upon the removal of Runs 284 and 287 it was found that the bag could not be reused because a band about one foot wide at the filament elevation was badly burned and cracked almost through the wall. In Runs 276 and 282, the sand had penetrated the elastomer nearly through the thickness in the band, but the elastomer was not heavily cracked or decomposed. However, the bag could not be reused. During this first series of pressure runs no particular operating difficulties were noted either with the vessel system nor the bag seals.

The power level during the pressure cycle in this test series is summarized in Table 8.

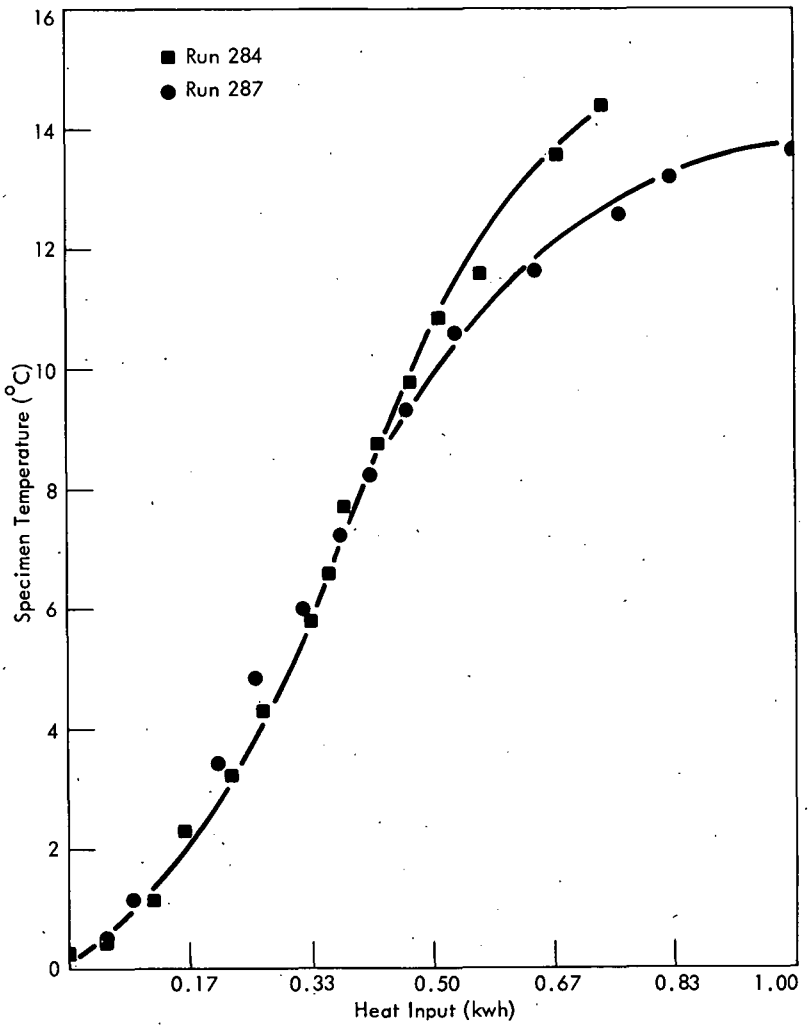

Figure 27. SPECIMEN HEATING CURVE AT ATMOSPHERIC PRESSURE.

As indicated, filament burnout occurs at about 10 kilowatts. This value corresponds to 100 watts/in^2 of heating surface. Thus, the heating rate and ceiling temperature for this configuration are limited unless a more refractory element, such as tungsten, is employed. The allowable heat flux for tungsten has not been determined. Tungsten coils are completely stable at 14 kilowatts, or 140 watts/in^2. This level is the limit of the existing power supply.

Examination of the used bags also disclosed that the skin temperature should be kept below 100° C at room pressure or 40° C at 15,000 psi or else the bag cannot be reused. Therefore, under these conditions pressure runs must be conducted such that power levels less then ten kilowatts and heat inputs less than two kilowatt hours are maintained.

Some improvement in the allowable heat input was obtained by inserting heat shields. The shields were ten-mil-thick cylinders of stainless steel either six or eight inches

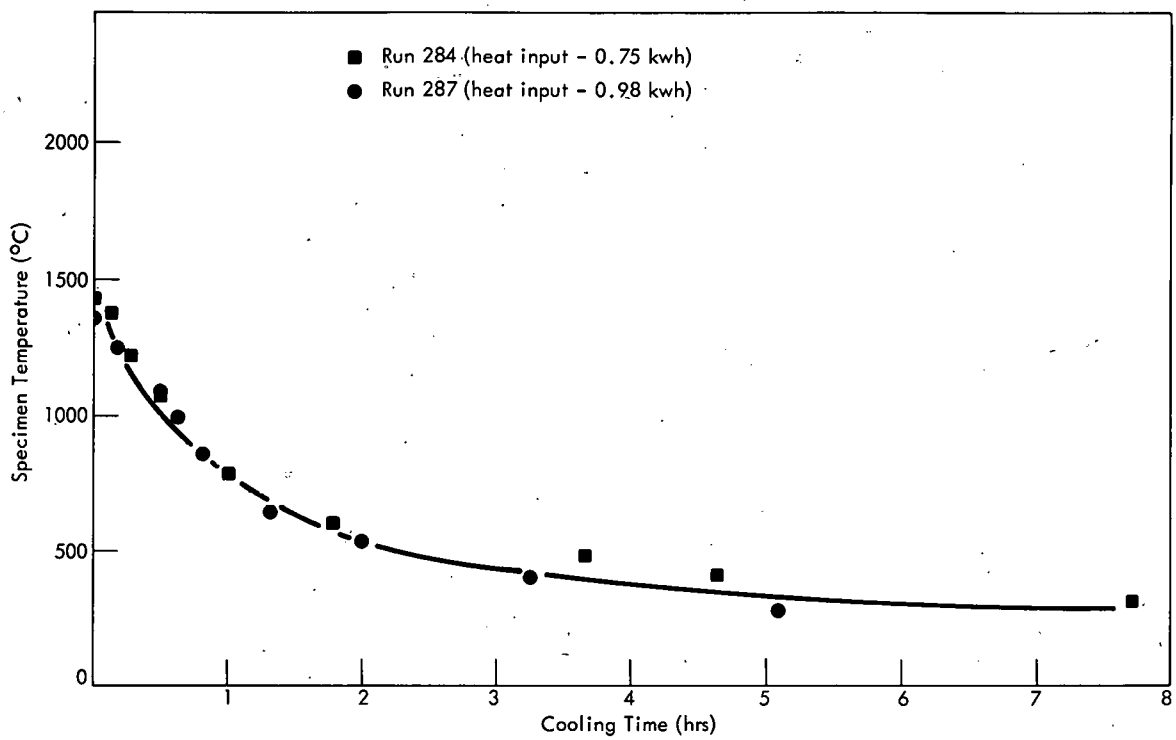

Figure 28. SPECIMEN COOLING CURVE AT ATMOSPHERIC PRESSURE.

in diameter and 24 inches long. The bag wall was further protected by covering in successive runs with mica, quartz, cloth, neoprene, and finally with silicone rubber. With these improvements, a 50% increase in the allowable heat input to three kilowatt hours was developed. The bag cracking is believed somehow to be related to the outgassing under heat and vacuum. This relationship was suggested by the fact that the same elastomer has been used in oil at 150° C under pressure over long periods without cracking or other signs of decay. It was learned that doping the inside of the bag with a nonhardening elastomer when gluing in the quartz, neoprene, or silicone protective liners eliminated the cracking.

In order to increase the allowable heat input above three kilowatt hours, the insertion of a heat sink at the bag skin was evaluated. Liners of lead that were 1/4 to 3/4 inch thick were used and the allowable heat input was indeed increased. In addition, the lead completely eliminated the intrusion of the sand into the polymer. The lead was obtained in 1/4-inch-thick sheets that were three by six feet in size. Each sheet was easily reusable. It was learned that with this configuration the allowable skin temperature could be raised to the elastomer curing temperature of 180° C. Results of this test series are indicated by the graph in Figure 34. The bags from all these test runs were found to be reusable. Although the weight of lead was not optimized, the 500-pound loading is close to the best value for this configuration. The allowable heat input under these conditions is 5 - 5.5 kilowatt hours. The effect of the liner on the bag surface temperature cycle is shown more clearly in Figure 35. Three experiments were run at a fixed heat input of 3 1/3

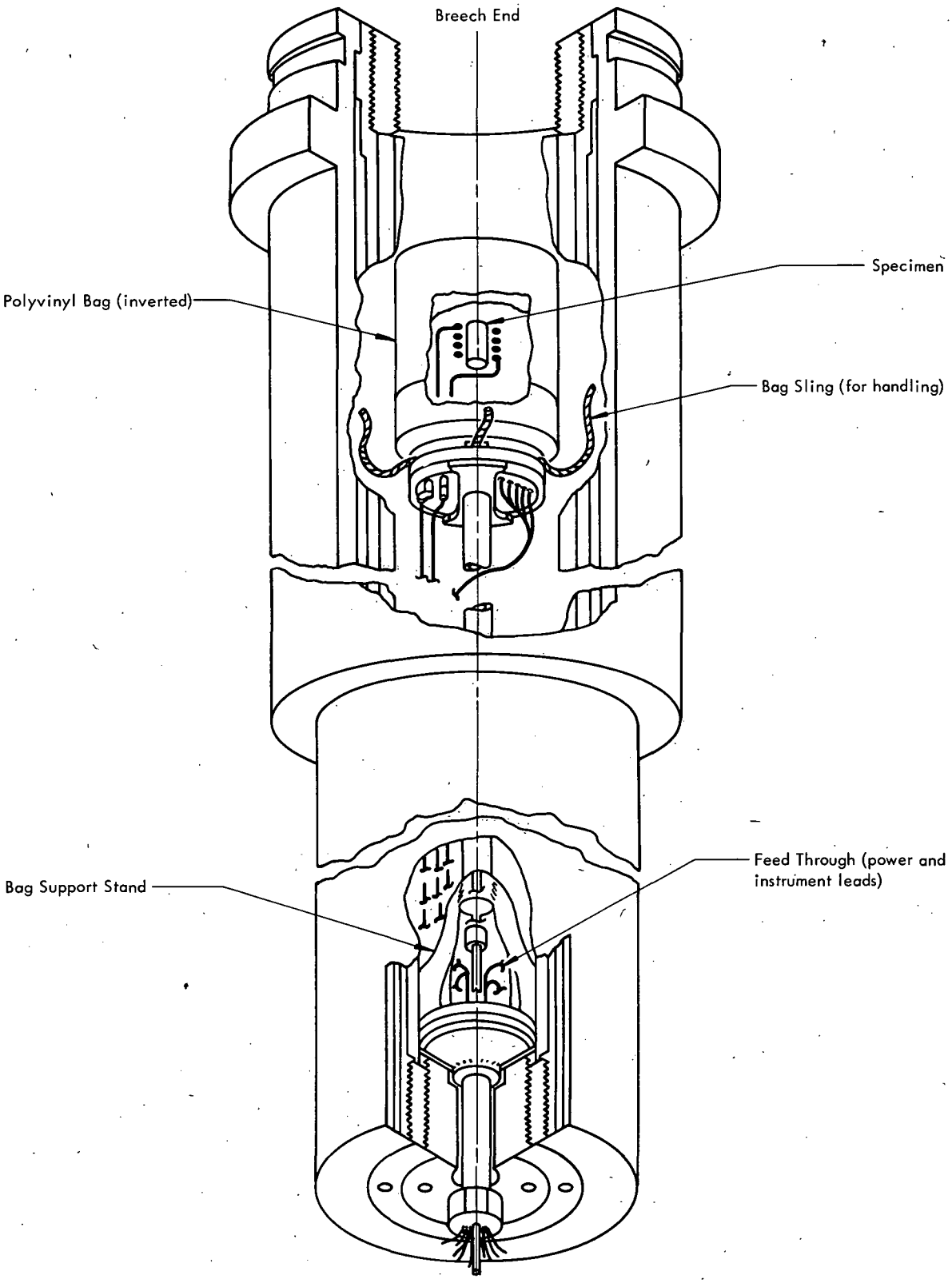

Figure 29. VIEW OF THE SIXTEEN-INCH PRESSURE VESSEL SHOWING THE INVERTED BAG FOR THE HOT-PRESS EXPERIMENTS.

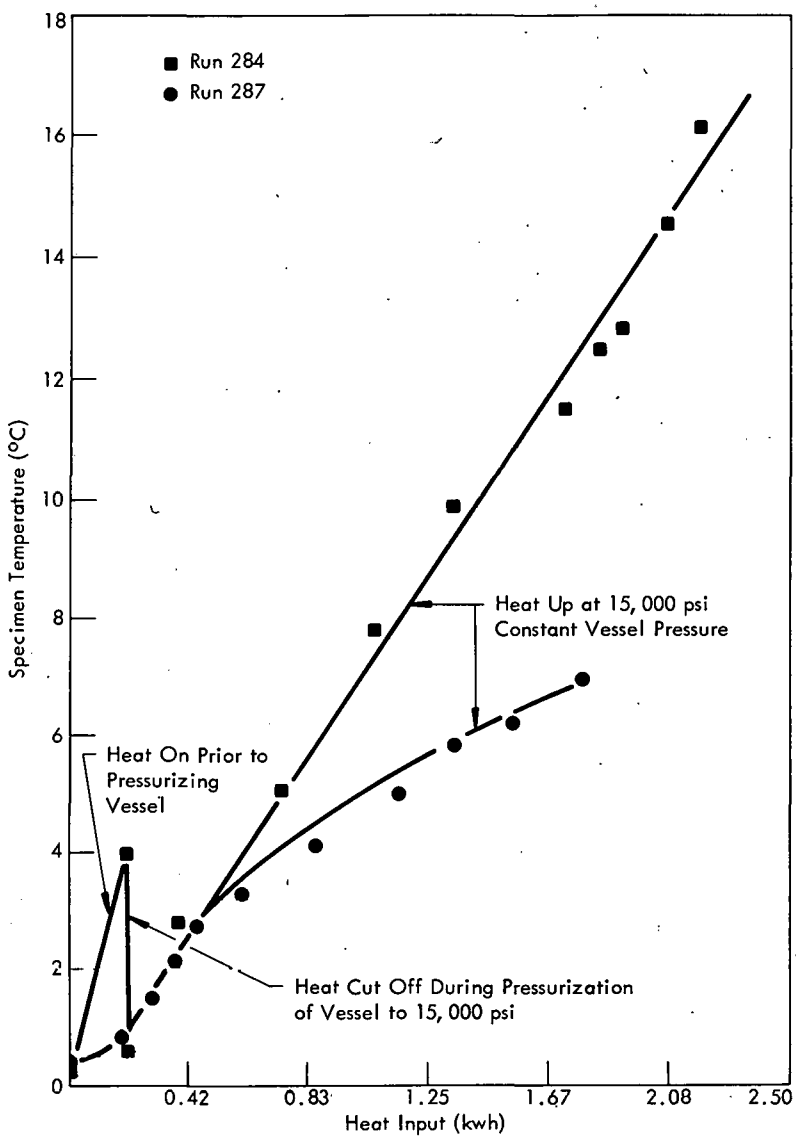

Figure 30. SPECIMEN HEATING CURVE FOR THE HOT-PRESS EXPERIMENTS.

kilowatt hours. The temperature cycle at the inner surface is shown without lead or pressure, and with a 200-pound lead shield both with and without pressure. As indicated, without lead or pressure a temperature peak of 175° C was reached in 6.6 hours. Using 200 pounds of lead against the inner skin, the temperature peak was only 71° C and 11.5 hours were required. When this configuration was used in a pressure run, a peak skin temperature of 124° C was obtained in 2.1 hours.

Over the period of evolution to the permissible 5 to 5.5 kilowatt hours input described in the preceding paragraph, it was learned that this level is generally independent of the specimen size and terminal temperature. The available soak time at a given temperature is, of course, dependent upon certain factors: by the limits

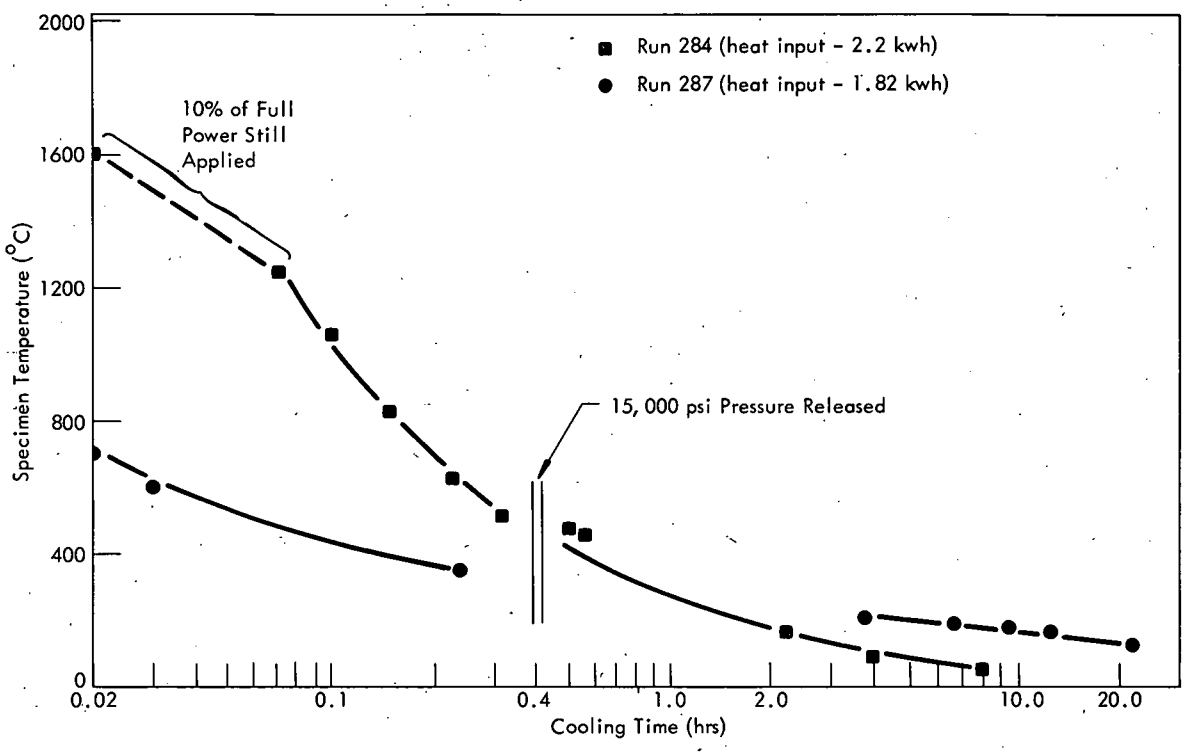

Figure 31. SPECIMEN TEMPERATURE DURING COOLING AS A FUNCTION OF TIME.

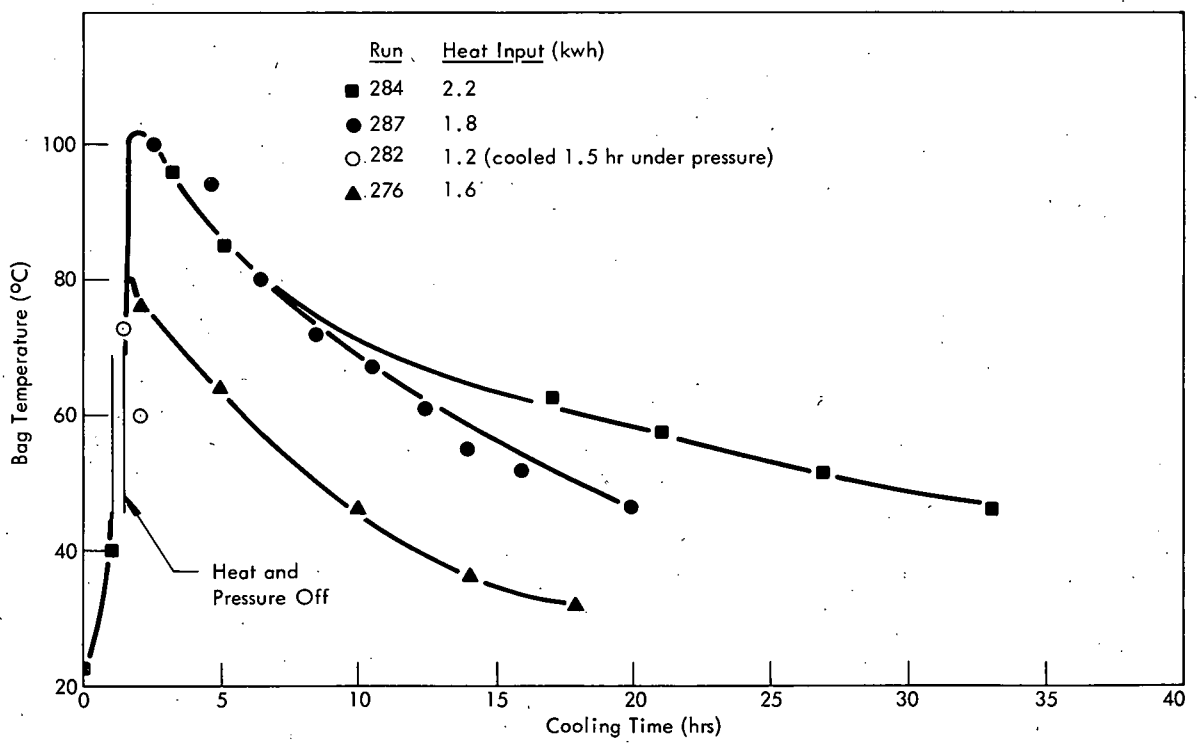

Figure 32. BAG WALL TEMPERATURE DURING HOT PRESSING AS A FUNCTION OF TIME.

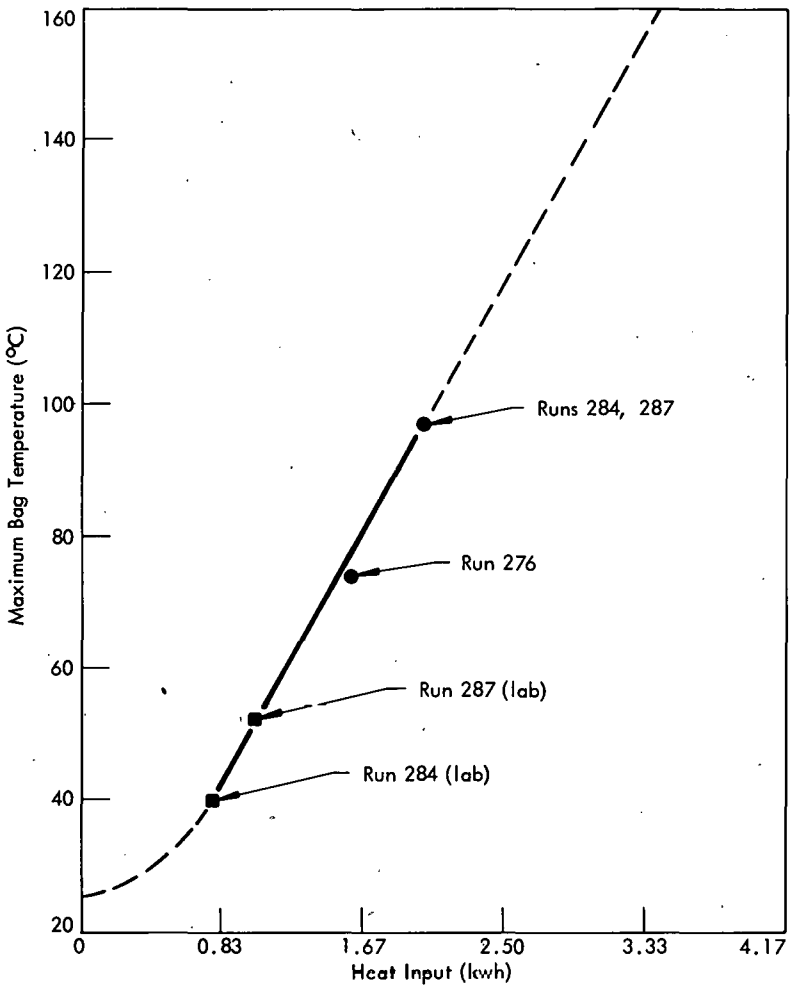

Figure 33. MAXIMUM BAG TEMPERATURE AS A FUNCTION OF THE HEAT INPUT.

Table 8

POWER LEVELS DURING PRESSURE CYCLES

	Run Number						
	277	279	280	282	283	284	287
Power Level (kwh)	13.1(1)	5.1	5.5	5.0	9.8	10.3(1)	12.5(1)

(1) Filament burnout caused termination of heating.

imposed by the maximum heating rate (10 kw) and by the limiting input (5 - 5.5 kilowatt hours). During the period a variety of specimens one to two inches in diameter and two to four inches long were pressed. The materials used and the conditions under which they were studied are very broadly summarized in Table 9. The metallography of several of the pressed bodies is of interest in that the specimens appear to be isotropic and fine grained. For example, the hot-pressed boron nitride generally available is obtained by graphite die hot pressing and is highly oriented. The

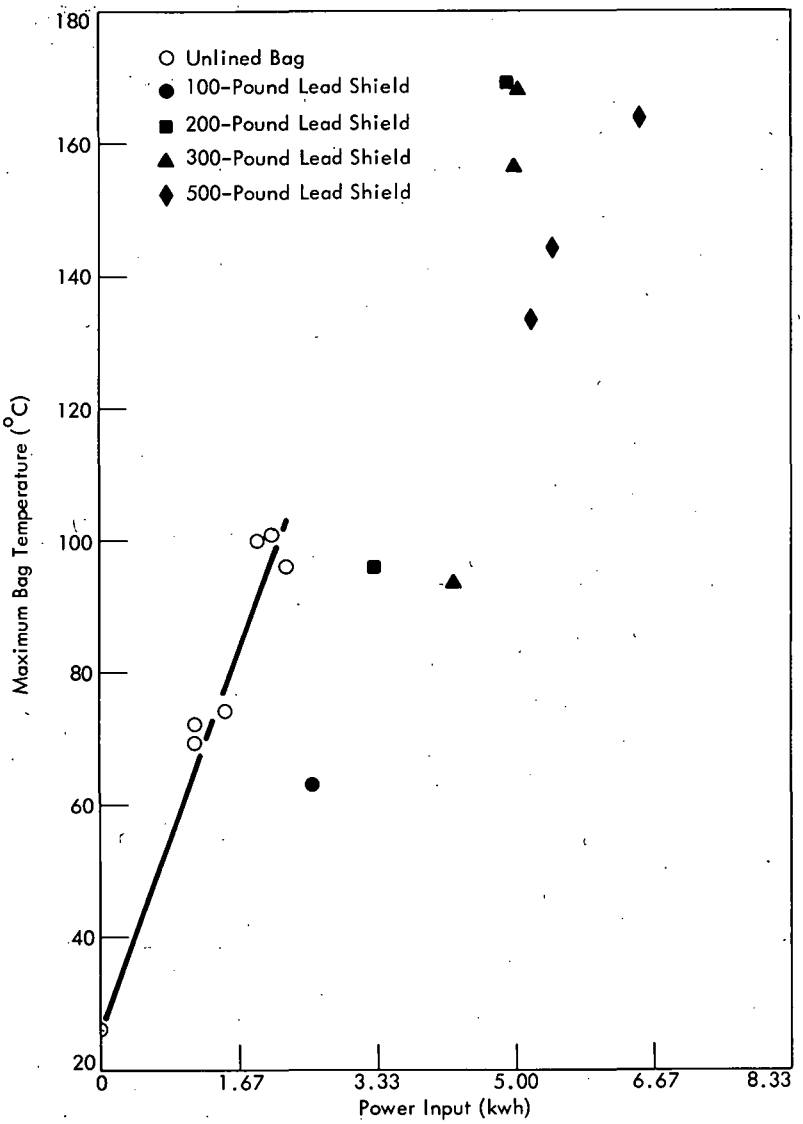

Figure 34. PEAK PLASTIC INNER SURFACE TEMPERATURE AS A FUNCTION OF THE HEAT INPUT.

boron nitride made in the isostatic press, shown in Figure 36(a), is 95% of the theoretical density (2.12 gms/cc). Uranium dioxide at a density of 10.9 gms/cc is 99.4% of the theoretical density. Photomicrographs of this material are shown in Figure 36(b) and (c). Pure tungsten was pressed to > 99% of the theoretical density, and is shown in Figure 36(d). Tungsten carbide bodies are normally prepared in a cobalt matrix because of the excellent binding obtained in this system. The hardest of these is about 1700 Knoop. A test in which the cobalt was replaced by 20 wt % tungsten for added refractoriness produced a body of 2000 Knoop. Single-crystal tungsten carbide hardness has been measured by French[10] to be 2400 Knoop at the basal plane and 1000 on the prism plane. Schwarzkopf[11] has reported the hardness of fused tungsten carbide to be 2000 Knoop. The pure tungsten carbide isostatically

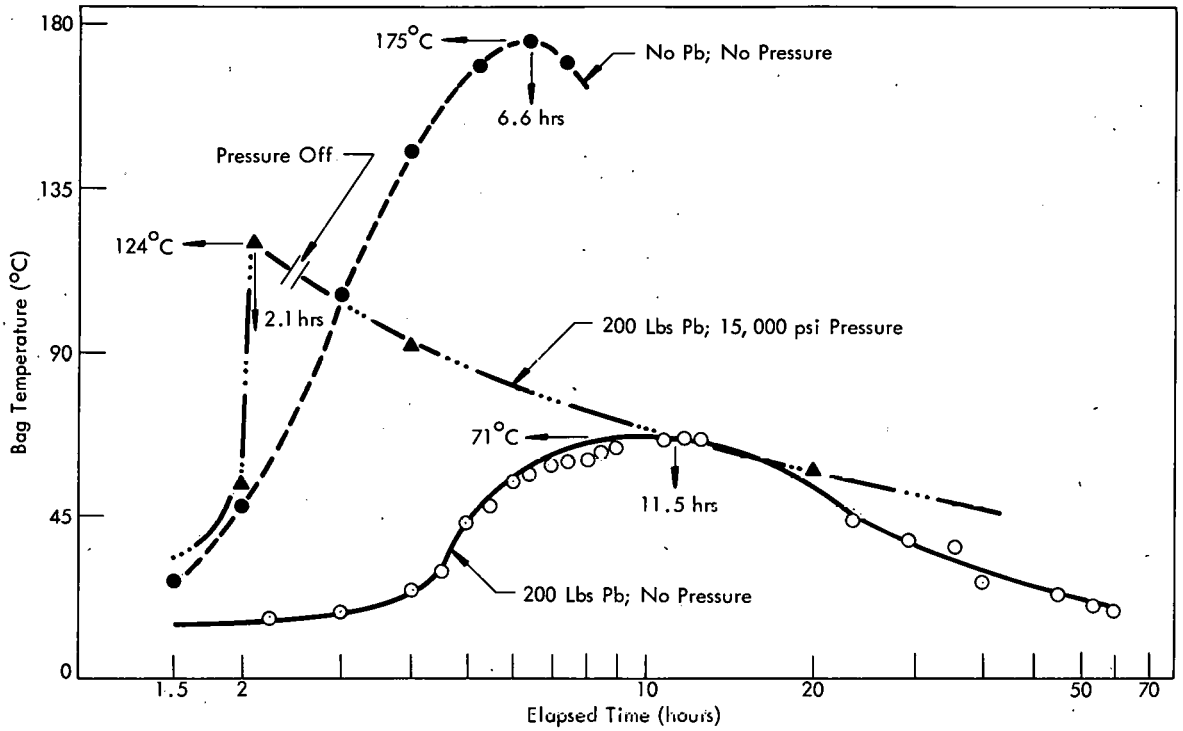

Figure 35. BAG INNER SURFACE TEMPERATURE AS A FUNCTION OF TIME. (Heat Input was 3 1/3 kwh)

hot pressed (Run 313, Table 9) was found to have an average Knoop of 2613. Sections of both materials are shown in Figure 36(e) and (f).

Metal Bag Evolution

The allowable heat input to the press system previously described has always been limited by the internal surface temperature of the polyvinyl containing bag. As originally conceived, the allowable input was two kilowatt hours. The deterioration was found to be delayed by doping and lining the inside surface and three kilowatt hours were realized. Subsequently, use of a lead heat sink (shield) in contact with the plastisol and other minor improvements raised this limit to five kilowatt hours. No further modifications promise to raise this substantially. However, one method of realizing a big increase is to replace the plastic bag altogether with an easily crushable and expendable metal bag.

A metal container (17" D x 0.020" T x 39" L) was rolled from oxygen-free copper stock. A bottom closure of the same material was cut and all closures were made by inert gas welding. A copper flange was made from the top which would fit the existing lid closures containing the electrical feedthroughs. The assembly was pressed (as shown for Run 328, Table 9) to a total heat input of 20 kilowatt hours instead of the usual five kilowatt hours. Although no limiting temperatures were even approached, the run was terminated to inspect the bag and, particularly, to determine whether or not the lid, the only plastic in the system, was overheating. Surprisingly, it was barely warm to the touch immediately after removal.

Table 9

SUMMARY OF EXPLORATORY HOT PRESSINGS AT 15,000 PSI IN PLASTISOL CONTAINERS

Run	Material Pressed	Insulation	Soak Time (min)	Temperature Range (° C)	Results
276 and 277	BN	MgO	8	1500	84% dense product.
284	$Al_2O_3 \cdot CoO \cdot Au$	BN	3	1600	Melted thermocouples.
287	$Al_2O_3 \cdot Cr_2O_3$	BN		1300	Melted thermocouples.
289	$Al_2O_3 \cdot CoO \cdot Au$	BN	5	1500 - 2000	
293	$BeO \cdot Al_2O_3 \cdot SiO_2$	BN	40	1100 - 1200	
294	$BeO \cdot Al_2O_3 \cdot SiO_2$	BN	20	900 - 1100	
295	75 wt % W-25 wt % Re	MgO	15	1650 - 1750	
296	75 wt % W-25 wt % Re	MgO	10	1800 - 1900	
297	Aluminum Ingot	MgO	35	> 700	Part retained shape after melting and solidification.
299	75 wt % W-25 wt % Re	MgO	15	1600 - 1800	
301	UO_2	BN	30	1400	
305	74 wt % W-26 wt % Re	MgO	15	> 2300	
306	W	UO_2	10	1500 - 1800	
307	W Powder (4 m^2/gm containing 1% O_2)	UO_2	25	1600 - 2100	Density - 88%.
308	BeO	MgO	54	1550 - 1800	Initial density 99%. Not improved.
311	CrB_2	BN	30	1700 - 1800	Evidence of oxidation.
312	74 wt % W-26 wt % Re (powder mixture)	UO_2	9	2300	Completely dense; not alloyed.
313	WC and WC-20 wt % W	UO_2	30	1800 - 2100	Good densification.
314	74 wt % W-26 wt % Re (prealloyed)	UO_2	26	2500 - 2900	UO_2 intruded the specimens.
319	90 wt % U-7.5 wt % Nb-2.5 wt % Zr	MgO	47	1100 - 1300	Part partially deformed.
323	W-26 Re:WC:W-26 Re	UO_2	17	est. 1800 - 2300	Completely dense.
324	BeO Canned in Ta	MgO	21	est. 1800 - 2000	Can and contents reacted.
325	$BeO:Al_2O_3:SiO_2$ (1:1:1)	MgO	25	1300 - 1400	Cooled 20°/min to 980° C.
328	MgO	MgO	90	2000 - 2600	See text, Page 43.

Thus, the allowable ceiling temperatures for the metal bag pressing system now become the maximum permissible temperatures for the pressing oil and for the pressure vessel itself. For the pressure vessel, operating at 30,000 psi, a longitudinal thermal stress from end to end induced by a temperature difference of 200° F would be acceptable. The allowable oil temperature is somewhat arbitrary; but since warm pressing at 150° C is regularly done, this limit is known to be acceptable. In the beginning it was planned to run the experiment until one of these limitations was approached. However, after more than two hours at over 1700° C and with four

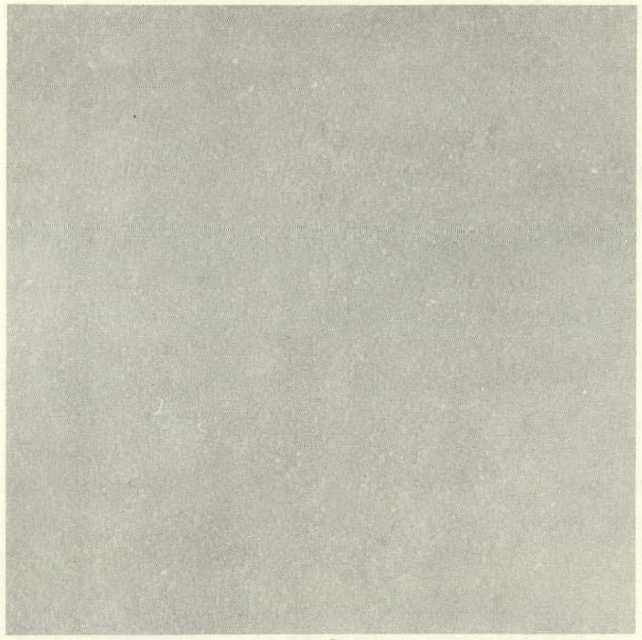

(a) BN 500X A754-1

(b) UO_2 A-765a

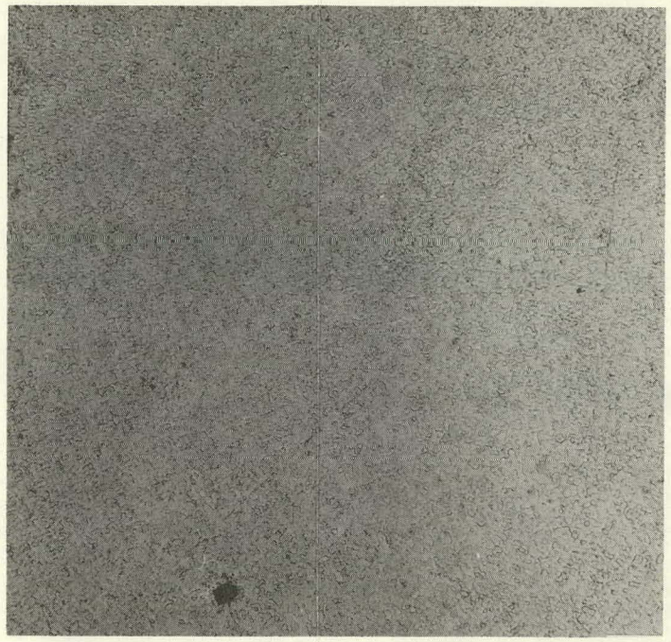

(c) UO_2, Etched A-765b

(d) W, Etched A897-1

(e) WC A-955-1a

(f) WC + 20 Wt % W A-955-2c

Figure 36. METALLOGRAPHIC SECTIONS OF SELECTED HOT ISOSTATICALLY PRESSED MATERIALS.
(100X Except as Noted; Bright Field Illumination)

times the usual heat input, neither of the limits was even approached, so the run was terminated. During the operation the copper bag surface temperature, the oil temperature in the annular space, and the pressure vessel inside surface temperature at the bag centerline were recorded. These results are plotted in Figure 37. Sufficient data to extrapolate to the steady-state temperature for the ten-kilowatt input were not obtained. However, some indication is implied in the data of Figure 38 for which the limit taken was 70° C. This temperature is equivalent to an overall metal-to-oil heat transfer coefficient of 20 Btu/hr-ft^2-°F. The copper then would stabilize below 200° C and the oil below 100° C. Immediately after pressing, the oil at the upper surface was 50° C and at the bottom was 23° C. Twenty-four hours after pressing, the copper surface was too hot to touch, and after 48 hours of cooling the surface was still warm to the touch. A photograph of the copper container after pressing is presented in Figure 39. The uniform collapse of the bag wall is clearly shown in the myriad of fine wrinkles with no noticeable distortion. The container shrank two inches in diameter and four inches in length. The magnesia boule from this run is shown in Figure 40. This run illustrates the extent of sintering for the

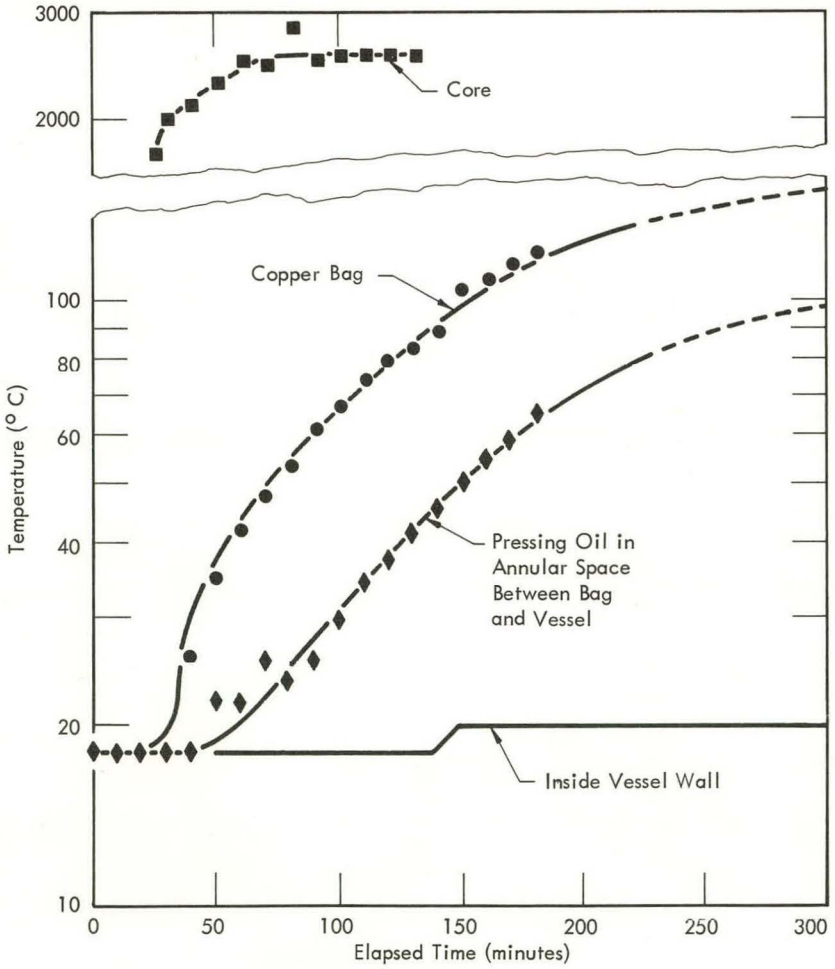

Figure 37. OIL, CORE, BAG, AND VESSEL TEMPERATURES AS FUNCTIONS OF THE ELAPSED TIME.

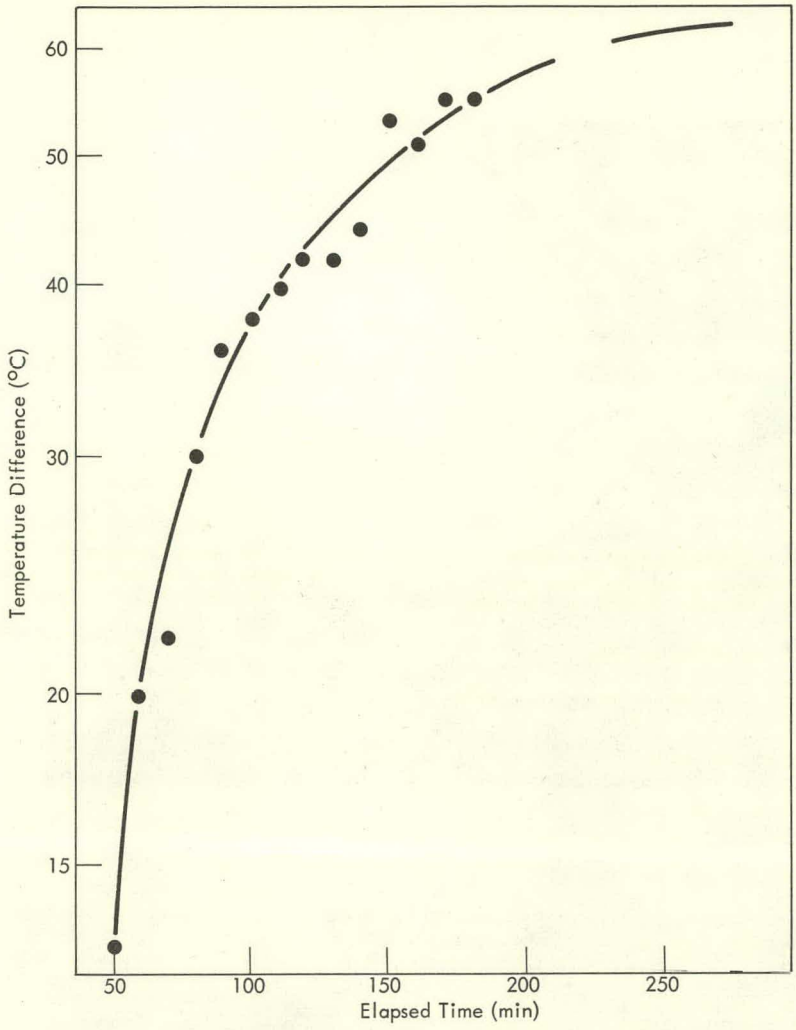

Figure 38. TEMPERATURE DIFFERENCE BETWEEN THE BAG SURFACE AND THE COOLING OIL AS A FUNCTION OF THE ELAPSED TIME.

given conditions. The heart of the boule is shown in Figure 41(a). The dark spot is the residue from a melted tungsten-rhenium thermocouple. An enlargement of a metal-free area is given in Figure 41(b). Its temperature experience is that plotted in Figure 37.

Although the overall shrinkage of these copper bags is partially dependent upon specimen shrinkage, the bulk of the permanent set is due to the crushing and densification of the sand. Crushing takes place in the cooler sand; permanent densification occurs in the boule. The initial metal bags were 16 1/4 inches in diameter and 38 inches long. During evacuation and outgassing, some wrinkling occurred depending upon how well tamped was the fill. Shrinkage results from several pressed bags are listed in Table 10.

114897(U)

Figure 39. COPPER HOT-PRESSING BAG ASSEMBLY AFTER USAGE.

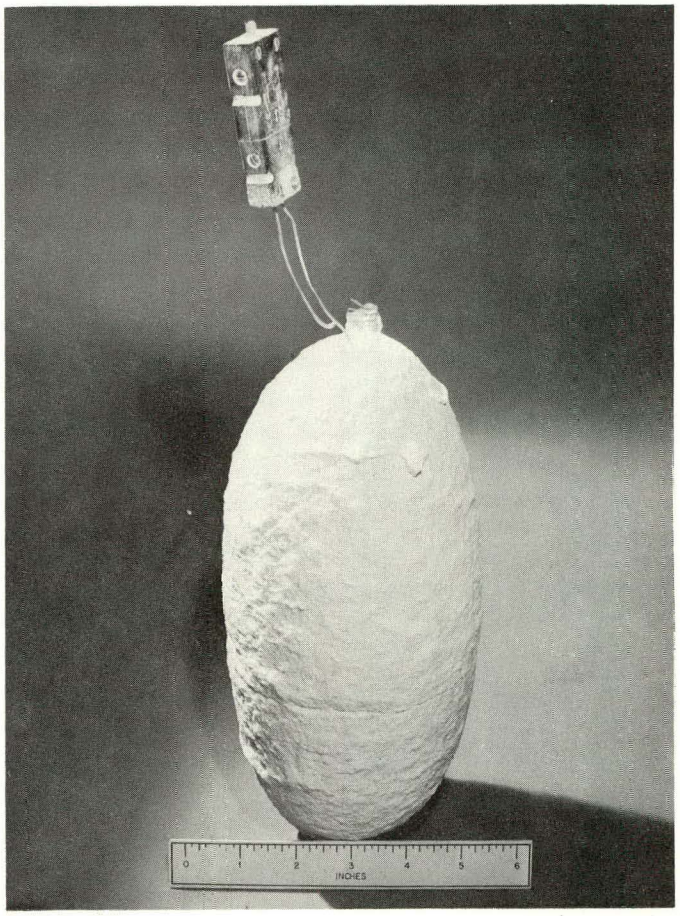

114896(U)

Figure 40. A MAGNESIA BOULE CONTAINING A 1 1/4-INCH-DIAMETER BY 5 X-INCH-LONG HEATING COIL AFTER BEING UNDER PRESSURE FOR TWO HOURS AT TEN KILO-WATTS.

(a) At 3.5X B-111-1

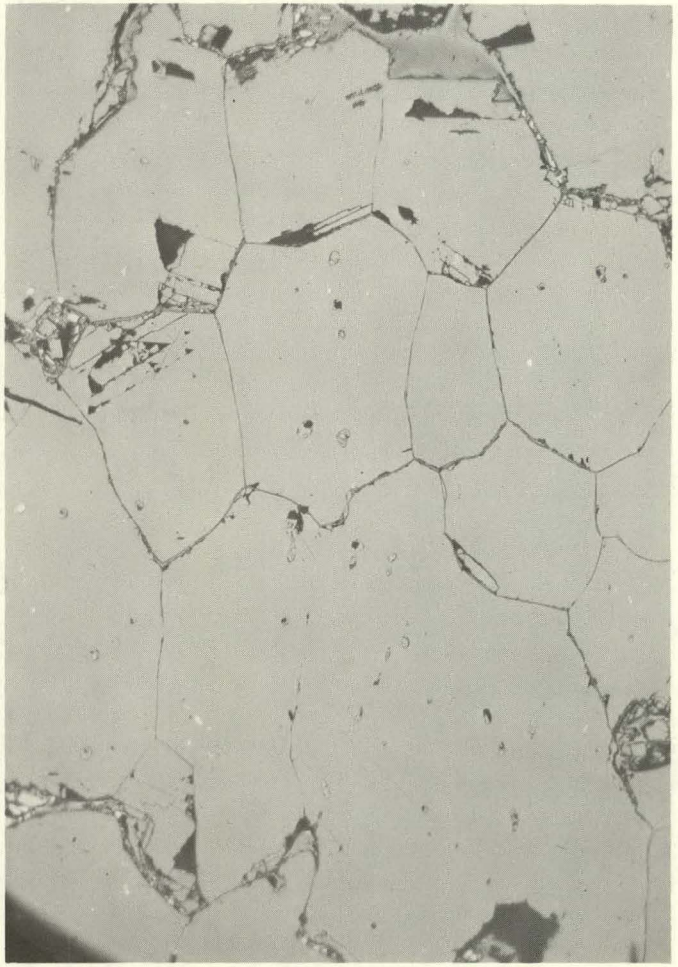

(b) At 75X B-111-2

Figure 41. METALLOGRAPHIC SECTIONS OF A MAGNESIA CORE AFTER HOT PRESSING.

Table 10

AMOUNT OF DIMETRAL AND LONGITUDINAL SHRINKAGE FOR BAGS OF VARIOUS SIZES

Diameter (in)	Shrinkage (%)	Length (inches)	Shrinkage (%)
14 1/2[1]	12	34 1/4	10
15 1/4	6	35 1/2	7
15 1/4	6	35 3/4	6
15	8	36	5
15[2]	8	36	5

(1) Lead bag.
(2) No specimen; all sand.

Although not significant, the diametral shrinkage appears, on the average, to be slightly greater than the longitudinal shrinkage. This is reminiscent of the uranium dioxide isostatic pressing experience brought out earlier in this report (Pages 19 - 26). The rubber bags are sufficiently resilient so that they are able to spring back very close to their original dimensions and are readily reusable. The lead liners used did not spring back and, in fact, their dimensions changed with each pressing. For instance, the lead liners were rolled from sheet 32 inches by 48 inches, but after pressing and unrolling the sheet, typical dimensions were 25 inches by 42 inches. The thickness increased about 50%.

The exploratory pressings made in the copper bags are summarized in Table 11. In the graphite pressings (Runs 331 and 335) heating was obtained by passing current directly through a 1/4-inch-diameter bar. However, this method was unsatisfactory because of the difficulty in temperature control. In the other runs listed there was no difficulty in heating or temperature control. In all runs listed, the bag seals were maintained and the collapse was smooth and uniform.

Large-Scale Experiments

The results reported in the preceding sections were all obtained in the 16-inch pressure vessel. Since the basic purpose of the study was to determine the feasibility of isostatic hot pressing on a large scale, and particularly since some prediction as to the capacity of the more recently acquired 60-inch vessel was required, exploratory experiments in a 30-inch vessel were undertaken to aid in determining the temperature, power, and size relation. In addition, the experience gained at this larger scale should provide an insight into any operating problems not noted on the 16-inch scale.

Unlike the 16-inch vessel of Figure 1, the 30-inch unit was equipped with an internal cooling jacket containing seven water paths of 22 gallons per minute each. Insertion of this water-cooled jacket lowered the vessel ID to 27 inches but provided the system with about 450 kilowatts of cooling for an 11° C temperature rise. The

Table 11

SUMMARY OUTLINE OF EXPLORATORY HOT PRESSINGS
AT 15,000 PSI IN COPPER CONTAINERS

Run	Material	Insulation	Soak Time (hrs)	Temperature Range (° C)	Results
328	None	MgO	2	2500	Established steady state load at 10 kw.
331	"JT" Graphite	MgO	30	2300	Not improved.
332	B_4C + 10 wt % B	MgO	0.2	1800 - 2000	
332a	SiC + 20 wt % Si	MgO	0.2	1800 - 2000	
333	74 wt % W-26 wt % Re	MgO	0.3	2300 - 3000	
335	"JT" Graphite	MgO			Burned out graphite conductor.
340	95 wt % W-3.5 wt % Ni-1.5 wt % Fe	MgO	2.0	1650	
341	$BeO:Al_2O_3:SiO_2$	BN	2.0	1500	Cooled at 1°/min for four hours.
342	74 wt % W-26 wt % Re	MgO	3.0	1900 - 2100	
343	LiH (canned in Type 304 SS)	MgO	3.0	400 - 500	
348	LiH (canned in Type 304 SS)	MgO	1.0	800 - 1100	

11° C figure was chosen to maintain longitudinal thermal stresses at a very low level. With the exception of the cooling jacket, the construction of the two units, including the breech openings, are quite similar. The vessel and its internal arrangement are diagramed in Figure 42. As indicated, power (provided through water-cooled leads) enters at the bottom; instrument leads feed in the top. There are four harnesses, each containing six pairs of leads that provide tungsten-rhenium and iron-constantin compensation.

The metal bag design and dimensions are shown in Figure 43. An adapting flange was provided so that the polyvinyl chloride lid used in the 16-inch work would fit. However, the neck produced at the top made filling and tamping difficult and could not be recommended for long-term usage. The heating filament in this work was formed from two each tungsten strips laid back to back. The strips had a width of one inch, a length of 144 inches, and were 0.020 inch thick. The ends were doubled for six inches to provide a low-temperature joint to the copper cable power leads. On the basis of the earlier work, this filament should handle over 50 kilowatts. As shown in Figure 43, four specimen thermocouples were used in the experiments. The test procedure was to develop steady-state conditions at a given power level and, after accumulating needed data, repeat the operation at several power levels. In all, four bags were pressed. The general data are summarized in Table 12.

Several operating difficulties arose that had not been experienced on the smaller scale. The intended power level in this work was 50 kilowatts. However, difficulty in balancing the voltage regulators feeding the low-voltage power supply limited stable operation to 25 kilowatts. Indeed, even with the 25 kilowatts available, it quickly developed that the steady-state power level was but 22 kilowatts because of hydraulic

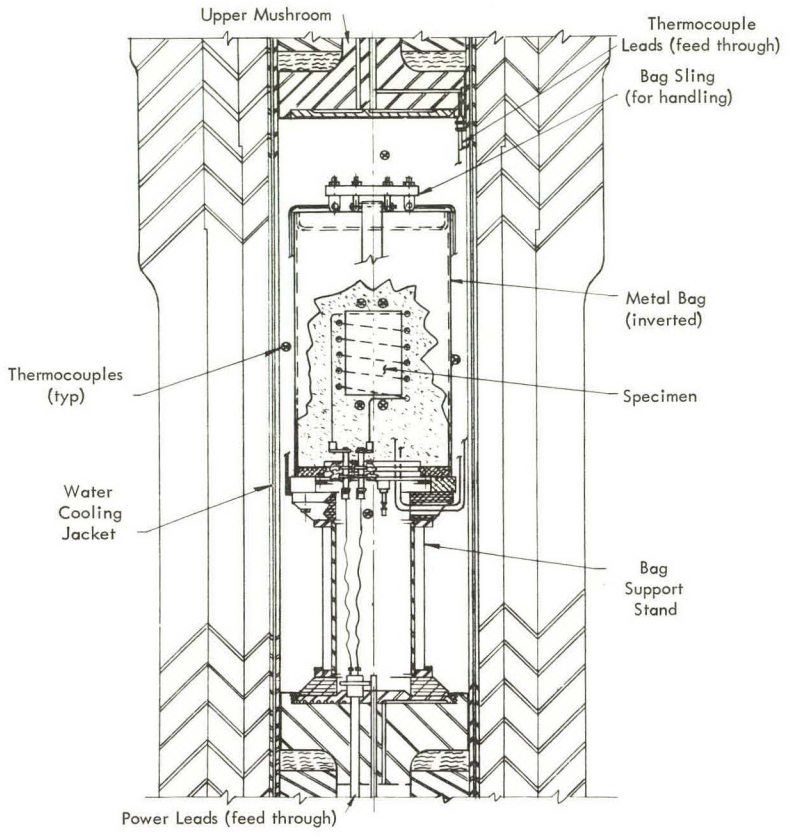

116245(U)

Figure 42. THIRTY-INCH PRESSURE VESSEL SHOWING THE HOT-PRESS SETUP FOR THE METAL BAG.

Table 12

GENERAL SUMMARY OF THE THIRTY-INCH PRESSING EXPERIMENTS AT 15,000 PSI

Run	Bag Material	Filament Dimensions		Pressed Material	Hydraulic Medium	Maximum Power (kw)	Remarks
		Diameter (inches)	Length (inches)				
344	Low-Oxygen Copper	6 1/2	12	5-Micron Tungsten Powder	Oil	9.4	Bag broke during pressurization. See text, Page 54.
345	Type 1100 Aluminum (dead soft)	8 1/2	12	25-Micron Tungsten Powder	Oil	25.1	
346	Type 1100 Aluminum (dead soft)	8 1/2	12	25-Micron Tungsten Powder	Water	22.4	First test using water for bag pressurization.
347	Type 1100 Aluminum (dead soft)	14	24	Steel Forging	Water	21	Bag broke during misoperation. See text, Page 55.

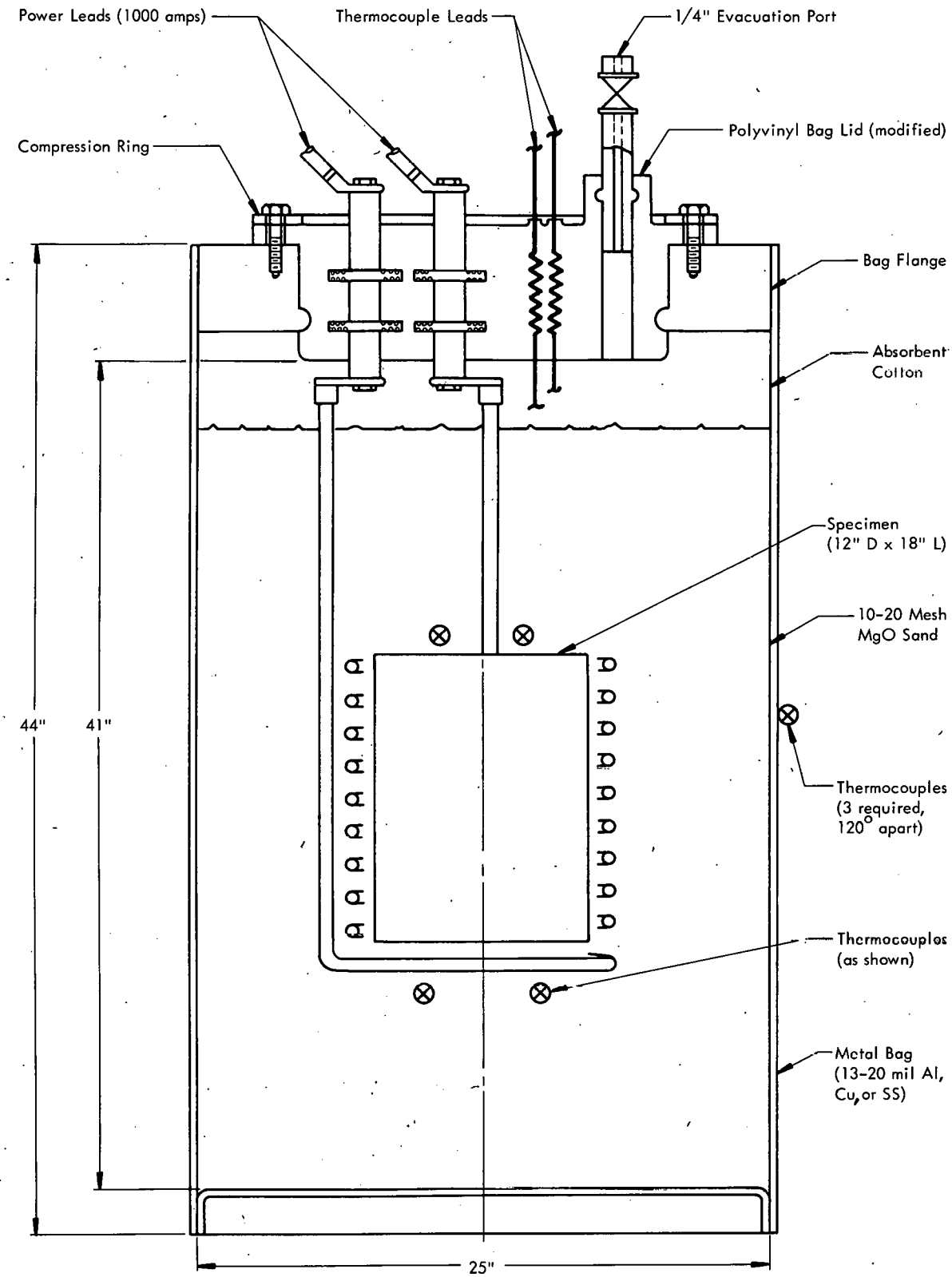

Figure 43. METAL BAG HOT-PRESS EXPERIMENT AS USED IN THE THIRTY-INCH PRESSURE VESSEL.

oil heating and cracking. Although in the small tests previously described (see Table 11) no leakage had ever occurred. This first 25-inch-diameter bag failed during pressurization. The failed bag was of low-oxygen copper not annealed after fabrication, while the earlier units were of oxygen-free, fully annealed copper. The bag failure was at the flange weld and the metal tore as it was stretched during pressurization. The tear extended over a 24-inch span, but very little sand was lost in removing the bag. A gradual increase in the filament current indicated that the failure had occurred. However, the rise was noted a full six hours prior to any decline in pressure. Upon first noting the pressure decline (~ 500 psi/hr), the power was dropped. In another eight hours the pressure had fallen to 10,000 psi. After opening the bag it was noted that the current increase was due to carbonaceous deposits around the filament. This oil-cracking process probably produces gas under sufficient pressure to prevent the free entry of fresh oil. Thus the pressure-decay process requires hours rather than being a sudden loss.

The second test (Run 345) revealed a power limitation of about 22 kilowatts steady state for the setup depicted in Figure 43. The average temperatures for 25-kilowatt operation are shown in Table 13. The mineral oil that is used degrades rapidly at 375° F (190° C) and this has been taken as the maximum allowable temperature. Since the water jacket remains at near 60° F, the very viscous oil in this region acts as an excellent insulator preventing heat removal by way of this path. From these results an overall heat transfer coefficient of 10.57 Btu/hr-ft^2-° F is obtained. A similar analysis of data from the 16-inch vessel develops a value of 11.5 Btu/hr-ft^2-° F and a maximum allowable power level of 14 kilowatts.

As a consequence of the serious power limitation that was experienced and in view of the available 450-kilowatt cooling capacity, an experiment was performed in which water rather than oil was used as the hydraulic medium (Run 346). Water, in addition to having a high heat capacity, has a much lower viscosity index (pressure and temperature) than oil, and water does not decompose at temperatures of interest. The water used was deionized and potassium chromate inhibited. The vessel was filled with water, the bag was immersed, and the closure made. The system was then pressurized in the usual way with oil which then collected at the breech. Only the oil was dumped prior to opening at the end of the experiment.

The steady-state temperatures are summarized in Table 13 along with those of the previous oil-immersion run for comparative purposes. Remember the layout of Figure 43 and the location of the thermocouples. As expected, a greater fraction of the heat load was removed at the jacket, as reflected in systematically higher exit water temperatures. In addition, the bag skin temperature remained much lower. Finally, the annular fluid ran at a very small temperature difference. Thus, while but 25 kilowatts were available for the test series, it is clear that water immersion will permit high power-level operation. An estimate of permissible levels is suggested in the discussion on Pages 62 and 63.

Table 13

TEMPERATURE SUMMARY OF RUN 345 (INPUT OF 25 KILOWATTS WITH OIL) AND RUN 346 (INPUT OF 22.4 KILOWATTS WITH WATER)

Water Entering Jacket	50° F at 2.2 ± 0.1 gpm						
Water Leaving Jacket							
Path Number	1	2	3	4	5	6	7
Temperature (° F)							
Run 345	59	58	58	56	59	58	58
Run 346	58	60	59	60	60	58	60

Bag Skin Temperature (avg ° F)	High	Middle	Low
Run 345	428	328	350
Run 346	90	175	-

Fluid in Annular Space			
Position	1	2	3
Temperature (avg ° F)			
Run 345	318	320	315
Run 346	140	100	-

Oil Above Bag, Just Below Breech Seal (avg ° F) 422

In the last run of the series (Run 347), a 13-inch-diameter steel forging was used to permit a study of the effect of a variation in specimen size along with the power for its effect on steady-state temperature. During loading, the bag was punctured and rewelded. It was subsequently pumped and found tight to helium. This experience served to illustrate that the 25-mil-thick aluminum in contact with sand can be repaired on the spot. The experiment went as planned and data at inputs of 11.8 and 21 kilowatts were obtained. Next, the input was raised to about 30 kilowatts, but while waiting for the steady state temperature, an emergency dump occurred. The cause of this pressure release could not be found. Since no indication of a pressure rise was noted, a valve malfunction appeared the most likely cause because the pressure decay occurred in a few seconds rather than over a fifteen-minute period as is normal. Upon repressurizing it was noted that the oil level was below the upper surface of the bag thus leaving the bag partially immersed in oil. The system was again depressurized and opened to pump off the oil. Finally, upon a third pressurization the bag sprang a leak shortly after reaching pressure. The leak was evidenced by a rapid pressure loss of over 1000 psi. The system was pumped to 15,000 psi and immediately a rise to 16,500 psi occurred. During this experience, the power level remained relatively constant. The pressure was bled to 15,000 psi and the fluctuation became more violent. At this point the run was terminated. Upon opening the system, the scene was one of great destruction. The bag was split at the bottom and several ripped openings at the top were left with ragged edges facing out. The lower tears did not noticeably point in. However, sand was spread all through the vessel and the bag was too distorted to lift out on its fixture. In the end, the sand was

sluiced away and the bag removed piecemeal. Despite the violence of the failure, the cleanup was completed in a single shift with no other interruptions to the work.

In summarizing the experience derived from the tests with the 25-inch-diameter bag, it was found that the bag shrinkage was about that for the 16-inch bag. Bag-shrinkage data are summarized in Table 14.

Table 14

AMOUNT OF SHRINKAGE WITH LARGE BAGS

Run Number	Diameter		Length	
	Initial (inches)	Final (inches)	Initial (inches)	Final (inches)
345	25	23 3/4	42 1/2	40
346	25	23	42 1/2	39

In these runs the shrinkage appeared uniform and no large sharp wrinkles were noted. A photograph of the bag from Run 345 as it was raised from the vessel is shown in Figure 44. Also shown is the lifting fixture and, in part, the power leads. The actual tungsten billet from Run 346 is shown in Figure 45. Some of the adhering sand after chipping away the boule is also shown. The steady-state data used in developing the temperature-size-heat input correlation are summarized in Table 15.

Table 15

STEADY-STATE SPECIMEN TEMPERATURE DATA OBTAINED IN THE TWENTY-FIVE-INCH-DIAMETER BAG TEST SERIES

Run	Steady State Input Power (kw)	Mean Specimen Temperature (° C)	Specimen Dimensions		System Pressure (psi)
			Diameter (inches)	Length (inches)	
344	1.2	1300	6	11	14.7
	9.4	960	6	11	15,000
345	14.8	920	8	10	15,000
	25.1	1750	8	10	15,000
346	15.0	1175	8	11	15,000
	22.4	2050	8	11	15,000
347	8.3	430	13	20	14.7
	11.8	260	13	20	15,000
	21.0	400	13	20	15,000
	32.0	750	13	20	15,000

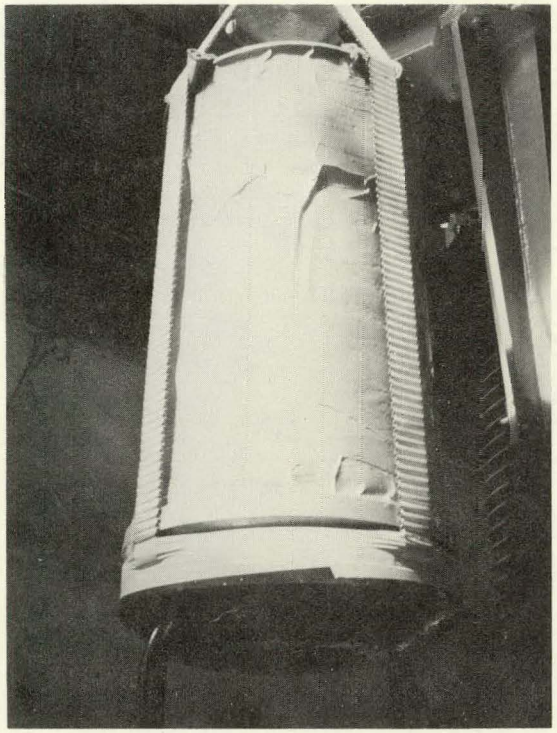

Figure 44. TWENTY-FIVE-INCH ALUMINUM BAG IMMEDIATELY AFTER PRESSING.

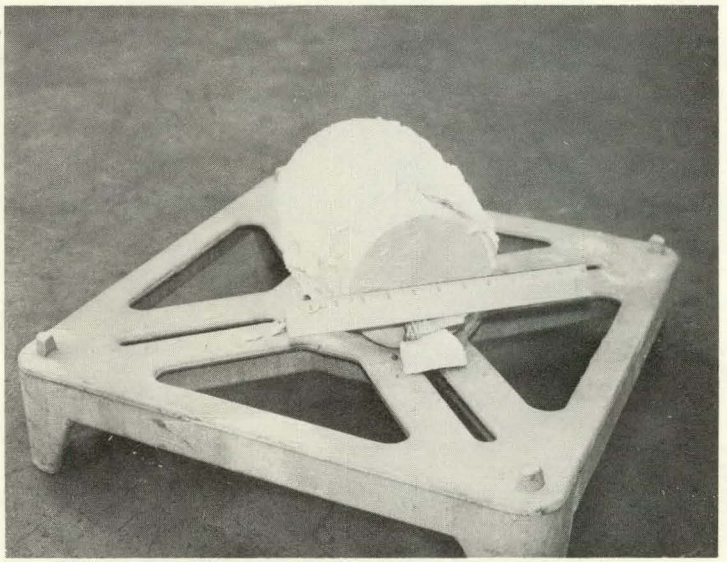

Figure 45. TUNGSTEN BILLET FROM RUN 346 AFTER CHIPPING AWAY THE BOULE.

THIS PAGE

WAS INTENTIONALLY

LEFT BLANK

DISCUSSION OF THE STUDY

EXPERIMENTAL RESULTS

Sand Pressure Transmission

The availability of a satisfactory sand, as previously brought out, is fundamental to the success of this hot-pressing process. The basic requirements are that it be nonforming, reusable, economical, isotropic in pressure transmission, and a good insulator.

Internally heated configurations have been used on a research scale for some time and have been described in detail by Hall[6-8] and others who have made general use of solids such as pryophyllite. However, these solids must be pressured to their fully plastic state before transmission efficiency becomes acceptable. Since the yield strength of pyrophyllite is ~ 3000 psi, pressure-transmission losses of about 50% would be sustained using a four-inch-diameter specimen in pyrophyllite in a typical layout such as shown in Figure 24 at a pressing pressure of 15,000 psi. Although transmission efficiences above 95% are generally reported, the operating pressures are always in the neighborhood of 1,000,000 psi. Solid pressing media such a pyrophyllite are unsuitable for large-scale work because of the difficulty and expense in preparing the part, and in machining out the pressed part.

At the outset, interest was centered in finding a sand of sufficient strength to withstand pressing pressures to 30,000 psi with a minimum of attrition. At room temperature, hydrostatic pressings of 3/4-inch-diameter compacts of magnesia, silica, alumina, and uranium dioxide from 8 - 100 mesh were nonforming to 300,000 psi. That is, noncoherent compacts were obtained. Cylinders, 14 inches in diameter, were pressed at 30,000 psi and the resultant mass was not found coherent, but a fines generation of about 5 wt % was noted. Since all these sands are relatively good insulators, exploratory pressure-transmission studies were made.

The method described previously was chosen because it approximates conditions prevailing in an actual pressing. The arrangement is shown in Figure 12 and involves pressing a uranium dioxide compact in the candidate sand and comparing the resultant density with that obtained by direct hydrostatic pressure. At the outset, a substantial enhancement in hydrostatic pressure appeared to develop. However, uranium and other powders such as magnesia and alumina in sinterable form were found to densify when repressed at a given pressure. Since a coherent shape must be formed prior to the sand press, it was necessary to adjust the data for the number of pressings the part experienced. Although significant density increases can be obtained by multiple pressing and by pressing in the various sands, after a single repress and particularly at pressures under 30,000 psi no systematic density increase could be resolved.

The full-scale uranium dioxide sand pressings carried out in cylinders do not show any density difference between oil and sand pressing (Figure 18). The final density of each pellet is reported in Table 3 and shows the apparent pressure uniformity. In spherical geometry (Figure 19) a distinct density loss was sustained and the matter was not studied further. A final demonstration of the degree of sand pressure transmission is shown in Figure 20 by reading the output of identical manganin coils, one in the hydraulic system and the other buried in the sand. The sand coil output rises with the hydraulic pressure but "holds back" during relief. However, the sand pressure does fully relieve, verifying that the sand is nonforming. Because of its ready availability, insulating value, and inertness, 4 - 8-mesh magnesium oxide sand was employed throughout the subsequent testing.

Plastisol Bag Experiments

The major difficulty in developing a plastisol bag for containing the hot press proved to be the designing of a dependable set of electrical feedthroughs. After this was accomplished, an assembly was soon developed which was dependable to five kilowatt hours of input. Table 9 lists the range of temperatures and soak times that were permitted for 1 1/2-inch-diameter specimens. Rubber or plastic compounds are not suitable container materials because of their inherently low conductivity. On the other hand, plastisols when under pressure are better insulators than the sand. The steady-state heat input under pressure was found to be less than two kilowatts. As a result, studies with metal bags were undertaken. The plastisol bags were reliable, however, and provided the hardware for the initial hot-pressing studies. From these, the practicability of the overall scheme was established. The bags were found to cost $148 to fabricate of which $40 was for material. The lids cost $19.80. Thus, when used for six runs the cost per run amounted to about $28.

Temperature Measurements

Temperature measurements have been based on the outputs of Pt/Pt-10 wt % Rh, W-26 wt %Re/W-3 wt % Re, and W-26 wt %Re/W-5 wt %Re thermocouples. Early experiments showed that the shifting sand during compression may shear fine wires and it was necessary to employ wires > 25 mils in diameter. Wires as fine as 10 mils and as coarse as 60 mils were tested. Platinum couples are readily reusable.

An interesting and useful property of platinum couples is that although they melt above 1750° C, once the pressure is on they are so closely confined that their output remains smooth. Upon cooling they do not show visual signs of having melted. These couples are generally surrounded by about 1/2 inch of fine sand, or boron nitride, although magnesia has also been successfully used. Since their output appeared smooth above the melting point, an experiment was performed in which the platinum couples were run contiguous with a W-26 wt % Re/W-3 wt % Re thermocouple inside a 1 1/2-inch-diameter tungsten heating coil. The established tungsten-rhenium calibration to 2250° C was used to extend the platinum-rhodium output to this level. Curves of the data are presented in Figure 46. The platinum-rhodium

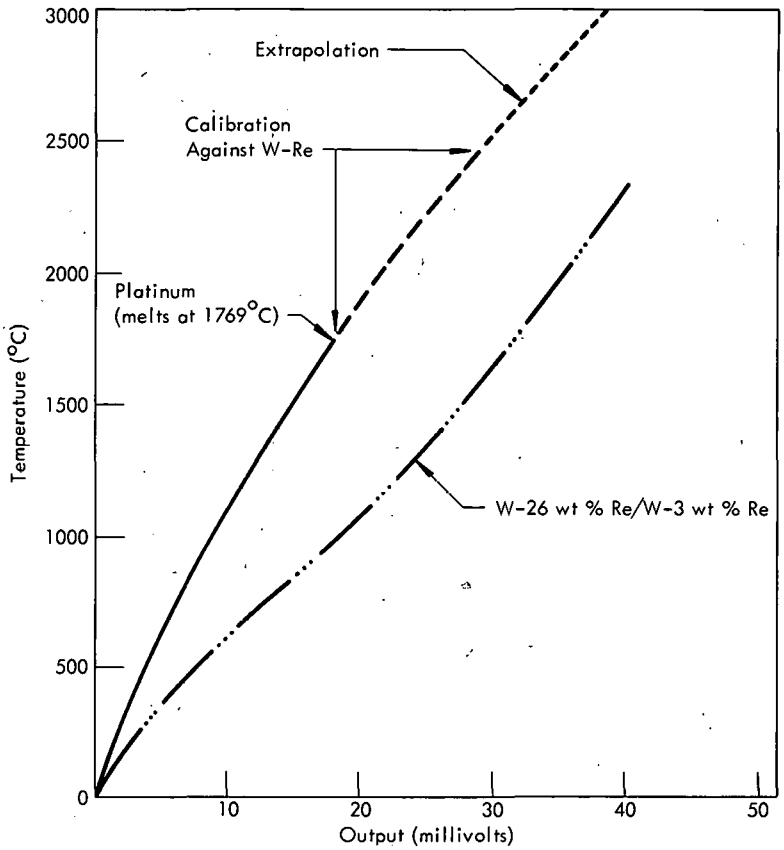

Figure 46. COMPARATIVE THERMOCOUPLE OUTPUTS UNDER 15,000 PSI SAND PRESSURE.

results have been extrapolated to 3000° C. Although the tungsten-rhenium couples become unstable above 2500° C, the platinum couples do not; and although the accuracy of the platinum couples in this range cannot be verified, they remain the only available estimate of temperatures above 2500° C.

Hall,[6] Birch,[12] and others have studied the decline in thermoelectric output of platinum thermocouples with increasing pressure. At pressures to 30,000 psi the effect is negligible.

Metal Bag Experiments

Metal bags of 15-mil-thick oxygen-free copper having about the same outside dimensions as the plastisol bags were modified so they could take the original plastisol lids. No mechanical difficulties arose. The bags were easily fabricated, filled, sealed, and opened. The limiting heat input of three kilowatt hours for plastisol bags was, of course, eliminated. The next power limitation (that of cracking the hydraulic oil) could not be precisely determined but was assumed to be about 14 kilowatts. As shown in Table 11, eleven successive runs in these metal bags were completed without difficulty.

The cost of producing these bags was $163.53 each as analyzed in Table 16. On the basis of the experience derived from the runs of Table 11, the overall cost of a single pressing would be $427.73. This analysis is itemized in Table 17.

Table 16

COST ANALYSIS FOR SIXTEEN-INCH COPPER BAGS

Work Materials		
Copper Sheet (25 mils)	$28.16	
Free Flange (100 uses)	0.28/Use	
Top Flange (3 uses)	34.40/Use	
Bottom Flange	16.22	
Total		$ 79.06
Labor		
Sheet Rolling (3/4 hr)	$ 7.50	
Free Flange Machining (3 hrs)	0.30/Use	
Top Flange Machining (8 hrs)	26.67/Use	
Bottom Flange Machining (2 hrs)	20.00	
Welding (2 hrs)	20.00	
Annealing (1 hr)	10.00	
Total		$ 84.47
Total Cost of Metal Bag Per Use		$163.53(1)

(1) Cost based on production in lots of two dozen each.

Large-Scale Tests

As brought out earlier, the primary project purpose was to develop an economical isostatic hot-pressing system for use in the 60-inch-diameter vessel. Although dependable and economical operation was achieved in the 16-inch vessel, and although even this accomplishment provides special capacity otherwise unavailable, still the extrapolation of these results to the 60-inch scale is too unreliable to be meaningful.

In an effort to obtain results at an intermediate level, four tests were made in the 30-inch vessel. The experiments were designed to provide data for defining the steady state temperature-power relation for pressing cylindrical shapes. In addition, some measure of the limiting heat input was desired.

It was found that the pressing oil cracks at 350° F (~ 175° C) generating hydrogen-containing gas. To maintain oil temperatures below this, the power ceiling was

Table 17

COST SUMMARY FOR A SINGLE PRESSING WHEN USING A SIXTEEN-INCH COPPER BAG

Bag Preparation			
Work Materials			
Bag Assembly (see Table 16)		$163.53	
Sand (MgO at 18 ¢/lb assuming a 10% loss)		5.40	
Filament (tungsten strip at $17.56/lb)		3.50	
Fittings and Cable		3.50	
Thermocouples and Connectors		36.00	
Lid and Feedthroughs (used 6 times)			
Material (40 ¢/lb)	$ 1.80/Use		
Labor (4 hrs)	12.00/Use		
Fittings	6.00/Use		
Subtotal		$ 19.80/Use	
Total			$231.73
Labor			
Filament Winding (2 hrs)		$ 18.00	
Bag Loading (3 hrs)		36.00	
Bag Testing (3 hrs)		36.00	
Total			$ 90.00
Total Bag Preparation Cost			$321.73
Pressing Operation			
Bag Pressing (4 hrs)		$ 88.00	
Bag Unloading and Sand Recovery (2 hrs)		18.00	
Total			$106.00
Overall Pressing Cost			$427.73

found to be 14 kilowatts for the 16-inch vessel assembly and 22 kilowatts for the 30-inch vessel. Data collected in both systems indicate overall heat-transfer coefficients of 11.5 and 10.6 Btu/hr-ft^2-$^\circ$ F, respectively. With water as the hydraulic medium, an overall coefficient of 45 Btu/hr-ft^2-$^\circ$ F was obtained at inputs of 10 - 30 kilowatts. However, since water does not decompose nor vaporize under the existing load conditions, operation at large temperature differences (viz, 800° F) should be feasible. The variation of the heat transfer coefficient with temperature difference was obtained by imposing the slope of Stoever's[13] results on that obtained in this work. The resulting correlation is shown in Figure 47. The basic value of 45 for the vessel system was derived from the results reported in Table 18 when the incoming water was assumed to be at 50° F.

The computed results are plotted in Figure 48 and, as indicated, a power level of one megawatt should be practical. The present cooling capacity is 0.450 megawatt which should dissipate at a Δt of 470° F.

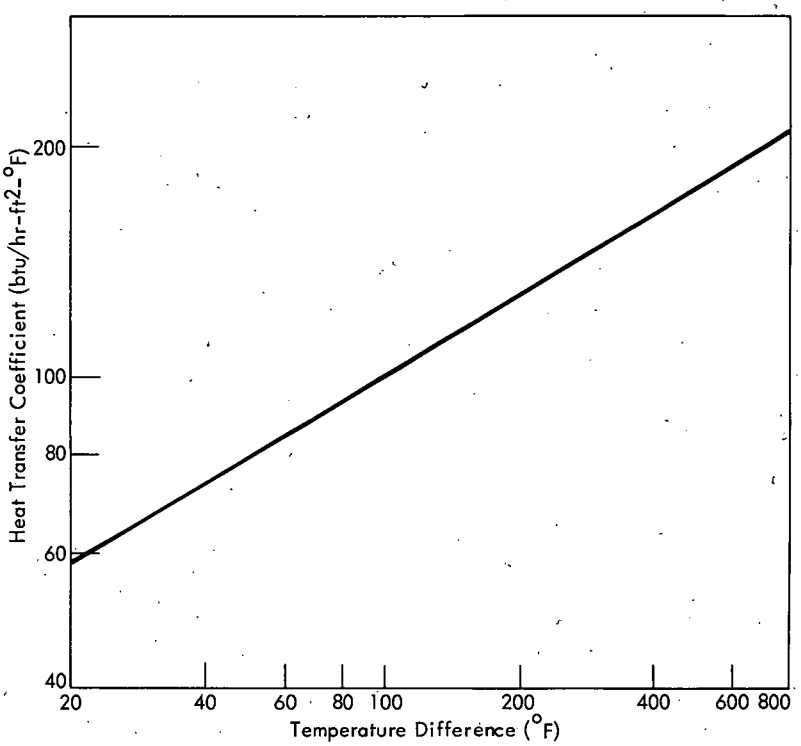

Figure 47. OVERALL HEAT TRANSFER AS A FUNCTION OF THE TEMPERATURE DIFFERENCE. (Water System)

Table 18

TEMPERATURE DIFFERENCES DURING THIRTY-INCH VESSEL RUNS

Run Number	Steady State Power (kwh)	Average Water Temperature (° F)	Average Skin Temperature (° F)	Δt Taken (° F)
346	22.4	120	132	72
346	15.0	112	110	62
347	11.8	130	120	72
347	21.0	140	180	120

OTHER CONSIDERATIONS

Correlative Model

The data from the large-scale tests, along with selected longer runs in the 16-inch vessel, can be employed to test the consistency of a correlative model containing the principal parameters as independent variables. Such a model, though not theoretically rigorous, has been developed.

A simplified sketch of the longitudinal section of the bag assembly presents the following pertinent nomenclature:

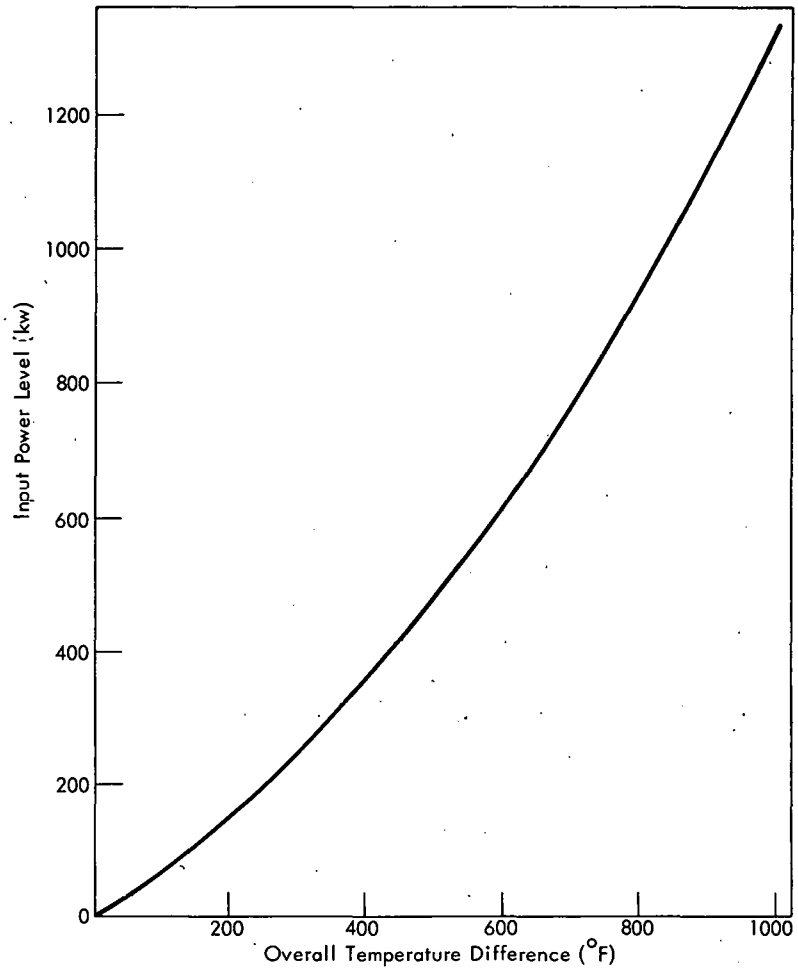

Figure 48. INPUT POWER FOR THE THIRTY-INCH PRESSURE VESSEL SYSTEM AS A FUNCTION OF THE BAG WALL-TO-COOLING WATER TEMPERATURE DIFFERENCE.

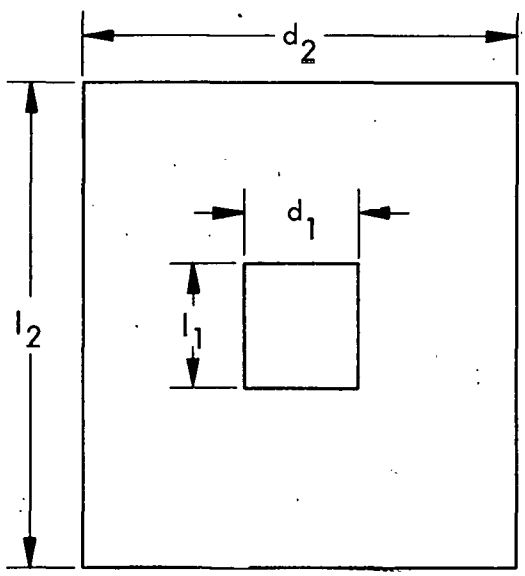

l_1, the coil length in inches,

l_2, the bag length in inches,

d_1, the specimen diameter in inches,

d_2, the bag diameter in inches. (These dimensions are taken after pressing.)

Δt, the temperature difference, specimen to bag skin in ° F,

k, the thermal conductivity in Btu/hr-in-° F,

q, the heat flow in Btu/hr, as indicated.

The Fourier equation for heat conduction is:

$$q = -kA \frac{dt}{dl}. \tag{1}$$

Where q (the heat flow value) is fixed and the isothermal area, A, is constant with respect to the length (l), the integral form for circular flats is:

$$q = \frac{k \pi d_1^2 (\Delta t)}{(4)(1/2)(l_2 - l_1)}, \tag{2}$$

and for concentric cylindrical surfaces it is:

$$q = \frac{k\, 2 \pi l_1 (\Delta t)}{\ln (d_2/d_1)}. \tag{3}$$

The specimen end losses can be approximated from Equation 2 and the peripheral losses from Equation 3 such that the integral loss becomes:

$$q = \frac{k \pi d_1^2 (\Delta t)}{2 (l_2 - l_1)} + \frac{k\, 2 \pi l_1 (\Delta t)}{\ln (d_2/d_1)} \text{ or,}$$

$$k = q/\pi \Delta t \frac{(l_2 - l_1)(\ln d_2/d_1)}{(d_1^2)(\ln d_2/d_1) + 2 l_1 (l_2 - l_1)}. \tag{4}$$

Using Equation 4 and the results from the three large-scale tests together with what steady-state data could be found in the 16-inch test results, an overall conductivity for the same can be computed. Given the range of test temperatures, power levels, specimen sizes, and the two bag sizes, the constancy of the resultant values should, therefore, be a sound test for the viability of the simplified model. The data employed are given in Table 19. The computed results using Equation 4 are also tabulated. The average thermal conductivity value was found to be 4.65 ± 1.9 (95% LE). This is an excellent correlation when it is realized that these data comprise a range of 3.9 - 32 kilowatts in power, 260 - 2050° C in temperature, 15 - 23 3/4 inches in bag diameter, 1 - 13 inches in specimen diameter, and 5 - 20 inches in specimen length.

The conductivity of magnesia is a function of its temperature. The conductivity of dense sintered material has been reported by Francl and Kingery[14] and McQuarrie,[15] and the data have been plotted (Figure 49). The conductivity of loose powder packs

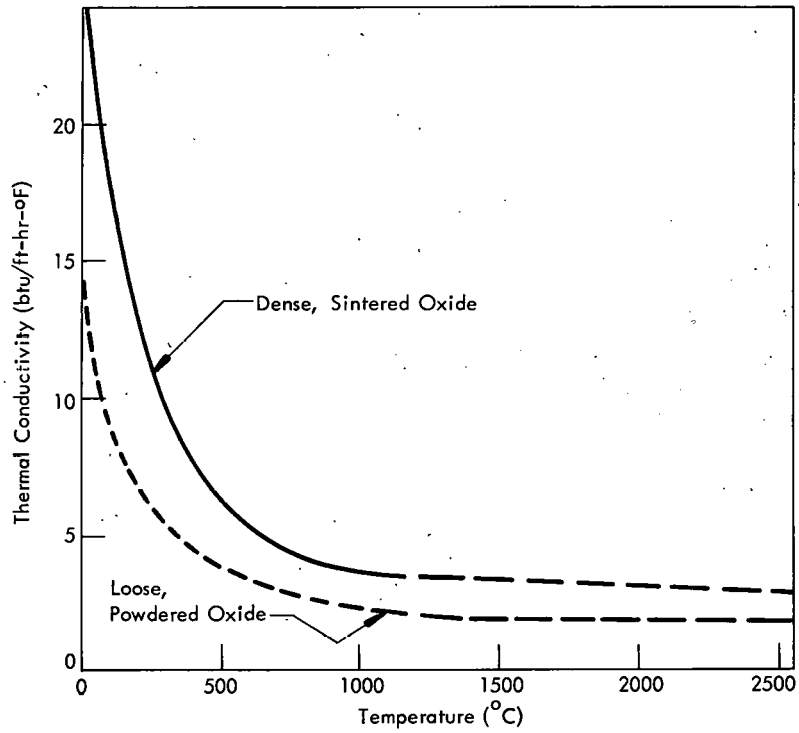

Figure 49. THERMAL CONDUCTIVITY OF POLYCRYSTALLINE MAGNESIUM OXIDE AS A FUNCTION OF THE TEMPERATURE. (From Francl and Kingery, and from McQuarrie)

Table 19

STEADY-STATE RUN SUMMARY DATA
OBTAINED AT 15,000 PSI

Run Number	Power (kw)	Mean Temperature (° C)	Bag Diameter (inches)	Specimen Diameter (inches)	Bag Length (inches)	Specimen Length (inches)	Computed k(1) (Btu/hr-in-° F)
328	10	2500	15	1	38	8	4.9
340	8	1670	15	2	38	6	5.6
341	3.9	1330	15	2 1/2	38	5	3.6
342	11.2	2000	15	2	38	6	6.6
348	10	900	15	8	38	10	4.3
344	9.4	960	23 3/4	6	40	11	4.0
345	25.1	1750	23 3/4	8	40	10	5.0
345	14.8	920	23 3/4	8	40	10	5.6
346	15	1175	23 3/4	8	40	11	4.1
346	22.4	2050	23 3/4	8	40	11	3.5
347	11.8	260	23 3/4	13	40	20	4.4
347	21	400	23 3/4	13	40	20	4.9
347	32	750	23 3/4	13	40	20	4.0

(1) Average - 4.65 ± 1.95 (95% LE).

has been reported at room temperature by Stoever[13] and is, of course, much lower than that for the dense material. The curvature for the dense material was used to shape loose powder providing the result shown in Figure 49. The area between the

curves is, therefore, the region of possible conductivity values over the pressure range. The average value of 4.65 obtained in this work corresponds to an average temperature for the insulating sand under pressure of from 400 to 700° C.

The computed conductivity can be used in conjunction with Equation 4 to develop the temperature-specimen diameter relationship in the 30-inch vessel for a given power input. Since there is presently available 450 kilowatts, the range of temperatures and specimen diameters of interest were computed and plotted (see Figure 50). Reference to Figure 48 shows that the bag wall would run at ~ 500° F. Given the available 450 kilowatts, cylinders from 17 3/4 to 19 3/4 inches in diameter could be pressed from 2500 to 1400° C, respectively. As expected, the ceiling temperature is very sensitive to the size of the cylinder.

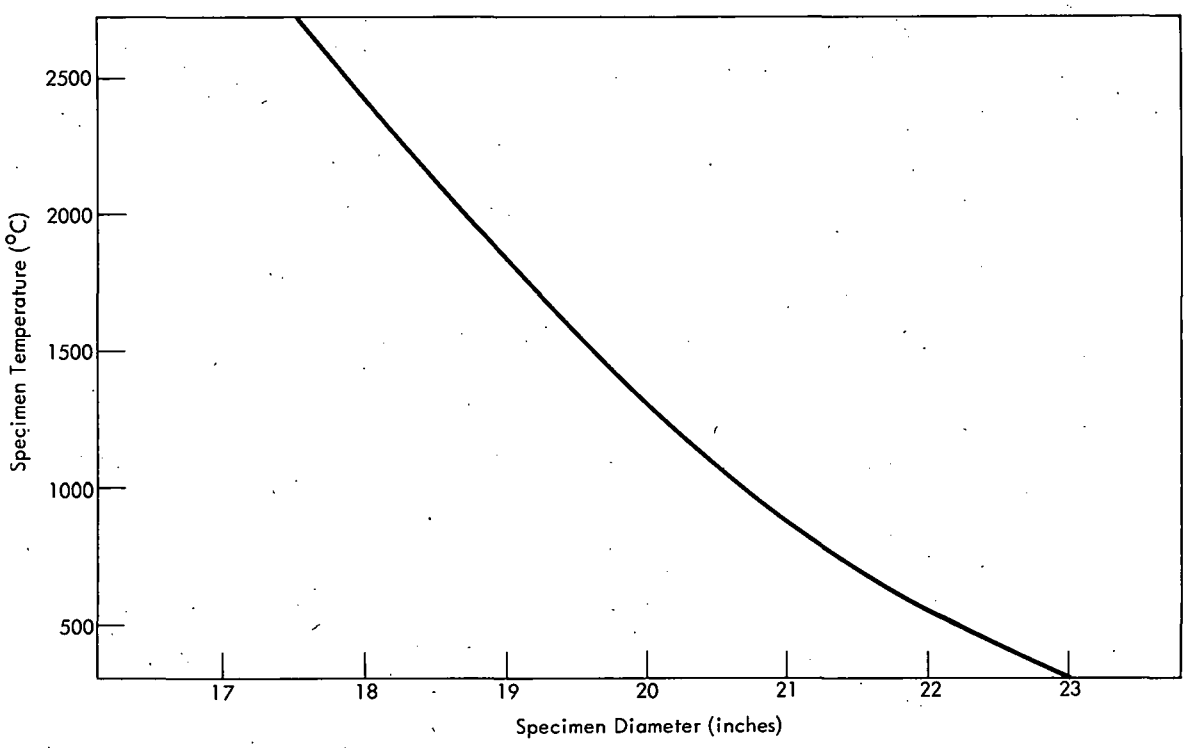

Figure 50. SPECIMEN TEMPERATURE AS A FUNCTION OF ITS DIAMETER. (Basis; 30" Work Hole; 450 kw Power; Specimen Length is Two Diameters; Bag is 27" x 53" L)

It is interesting to scale the 16-inch and 30-inch results to the 60-inch-diameter vessel. There is presently no water cooling available in the 60-inch vessel. Therefore, without cooling of any kind, the limiting power input, based on experience with the 16-inch vessel, would be about 100 kilowatts. With external water cooling it would be about 400 kilowatts, and with internal cooling it would be > 900 kilowatts. Since the 60-inch-diameter vessel is also 60 inches deep, a specimen having a length equal to its diameter was assumed for the computation. The temperature-specimen diameter relationship at 450 and 900 kilowatts input has been plotted

(Figure 51). At 2500° C, 35 and 40 1/4-inch-diameter compacts, respectively, could be pressed at these power levels. The power requirement-specimen diameter relation for two temperatures of interest (2500° C and 700° C) is shown in Figure 52.

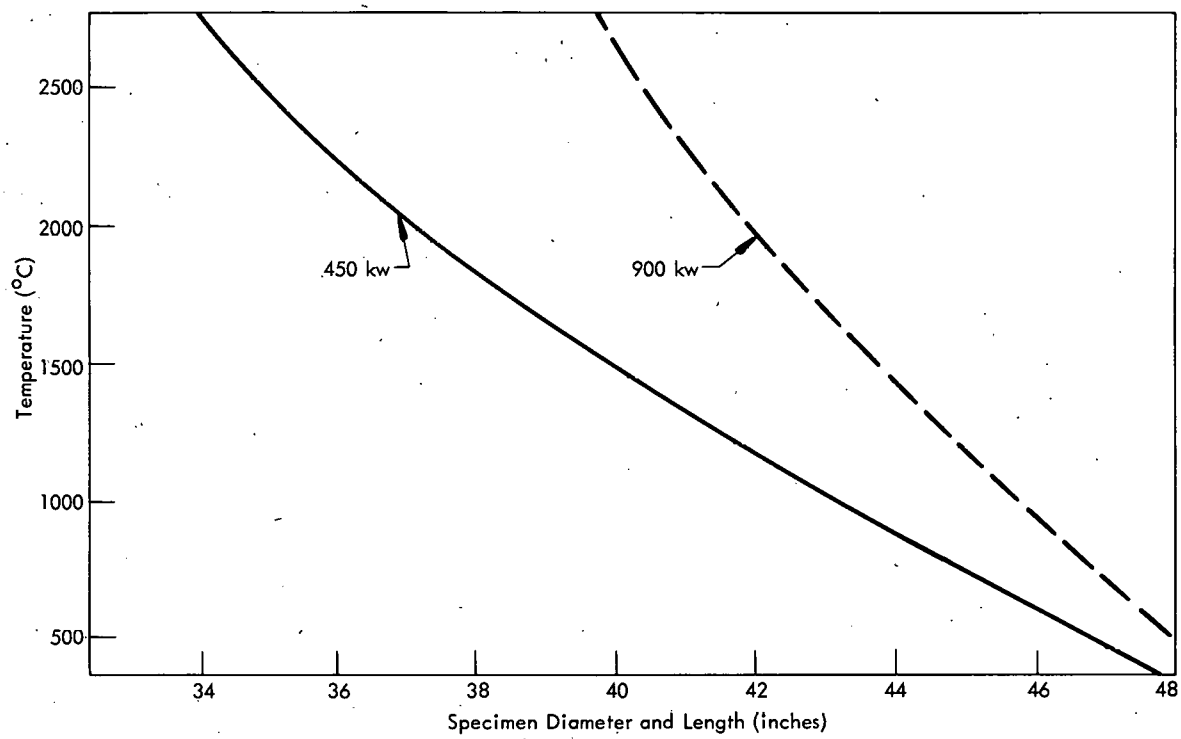

Figure 51. SPECIMEN TEMPERATURE AS A FUNCTION OF ITS DIAMETER. (Basis: 60" Work Hole; Specimen Length is Equal to its Diameter; Bag is 58" D x 58" L)

Improved Bag Design

In the experiments described to date, the 16-inch-diameter containing bags have been made of 20-mil-thick, oxygen-free, dead-soft copper. In no case was any mechanical difficulty experienced. Of the four 25-inch-diameter bags, the first was 25 mils in thickness and made of low-oxygen copper that was half hard, and it failed during operation. The three remaining 25-inch bags were made of 25-mil Type 1100ST aluminum that was fully annealed. One of the three leaked after three excursions to pressure. Since this experience, 16-inch bags of 25-mil annealed Type 304L stainless steel and 1/4-inch lead have been made and tested. Both materials behaved quite satisfactorily. A photograph of the lead and stainless units after a pressing run is presented in Figure 53. One lead bag was pressed with a two-

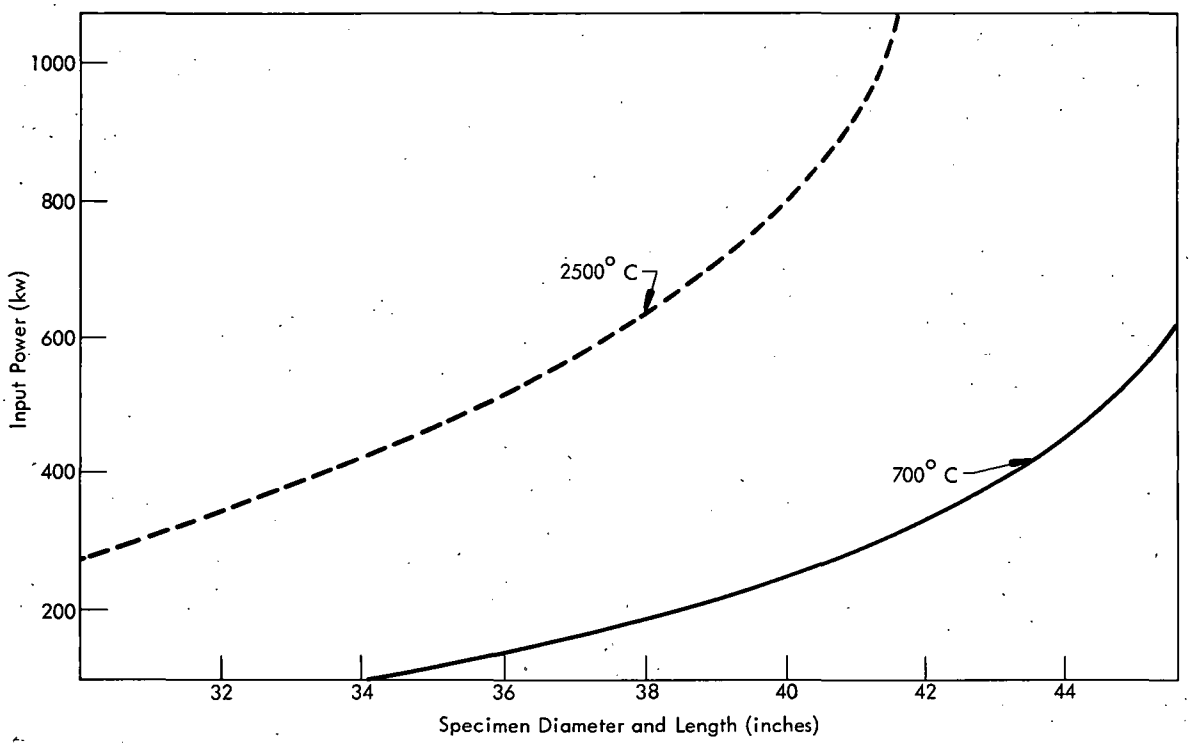

Figure 52. INPUT POWER AS A FUNCTION OF THE SPECIMEN SIZE FOR TWO TEMPERATURES. (Basis: 60" Work Hole; Specimen Length is Equal to its Diameter; Bag is 58" D x 58" L)

inch pipe as a specimen to create an extra large volume change during pressing. The lead bags show the most uniform shrinkage of all materials tested. Additionally, on a production manufacturing basis, the cost would be low because the lead could be cast and recovered. The dependability and cost of the various construction materials are listed in Table 20 with their preference ratings.

As suggested in the listing, for a pressing rate of about 4 to 5 units/day, the lead bags are the desired construction. Although they have not been produced in numbers sufficient to yield a dependable cost, they could likely be made for $75 each in quantities of four to six dozen. This unit cost would drop the presently calculated

Table 20

BAG CONSTRUCTION MATERIALS AND THEIR PREFERENCE RATINGS

Material	Fabrication Cost	Dependability	Remarks
O_2-Free Copper	2	2	Best material for limited production operation.
Low-O_2 Copper	2	4	Unacceptable.
Type 1100 ST Aluminum	4	3	Requires special welding equipment.
Type 304 L Stainless	3	2	Simplest for field fabrication.
Lead	1	1	Best material for large production rates.

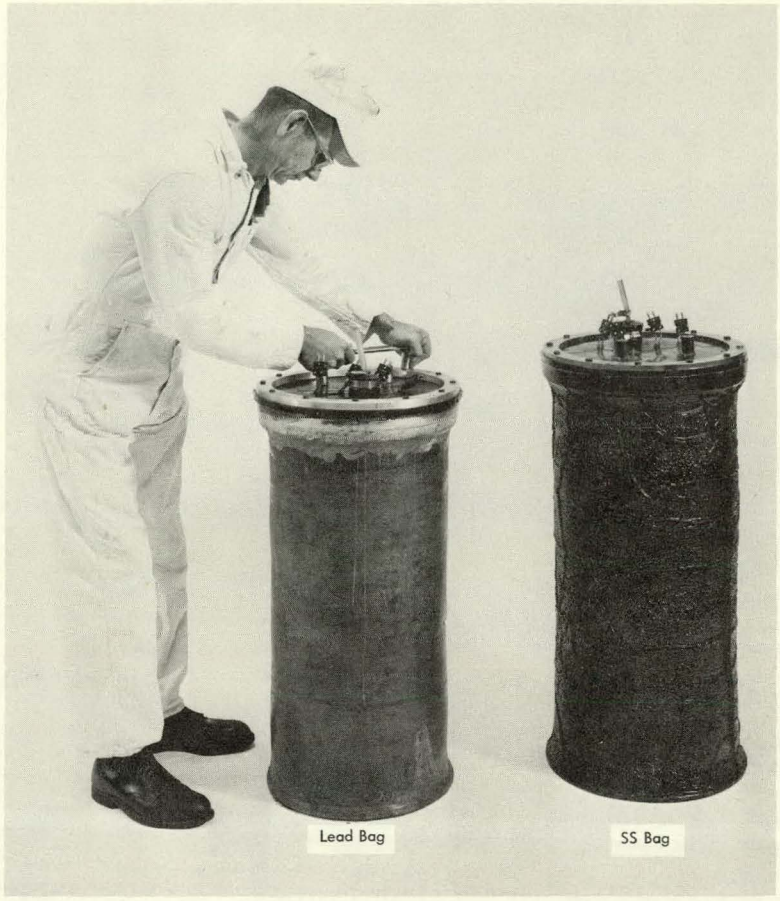

115981(U)

Figure 53. LEAD AND STAINLESS STEEL TEST BAGS AFTER HOT Pressing.

pressing cost shown in Table 17 to $271.73 per run. For production operations requiring one or less pressings a day, stainless steel is the preferred construction material.

THIS PAGE

WAS INTENTIONALLY

LEFT BLANK

CONCLUSIONS

Some essential conclusions can be made as a result of this study:

1. Routine operation with 16-inch-diameter bags has established that trouble-free isostatic hot pressing can be accomplished on this scale.

2. Experience to date on the 16-inch-diameter operating scale has shown that pressings of four-hour duration can presently be made for $427.73 each. By expanding operations this might be cut to $271.73 each.

3. Experiments at the 25-inch-diameter scale indicate there are no mechanical or operating problems arising from this increase in the scale of operations.

4. Data accumulated at the two operating levels have been utilized to estimate the capacity of the available 60-inch vessel if it is provided with the necessary cooling and power. Table 21 summarizes the results of this study.

Table 21

POSSIBLE CAPACITY OF SIXTY-INCH PRESSURE VESSEL COMPARED WITH KNOWN LIMITS OF SMALLER VESSELS

Vessel Diameter (inches)	Power (kw)	Temperature (° C)	Ceiling Pressure (psi)	Maximum Diameter of Pressing (inches)	Remarks
16	25	2500	30,000	3	Now in operation.
30	450	2500	20,000	17 1/2	Internally cooled vessel, and power supply available.
60	900	2500	30,000	40	Vessel available but requires cooling and power installation.

THIS PAGE

WAS INTENTIONALLY

LEFT BLANK

REFERENCES

(1) Newkirk, H. W. and Anicetti, R. J.; Bull Am Cer Soc, 37, p 471 (1958).

(2) Hodge, E. S., Boyer, C. B., and Orcutt, F. D.; "Gas Pressure Bonding", Ind and Eng Chem, 54, (1), p 31; January 1962.

(3) "Gas Pressure Bonding", DMIC-159; September 25, 1961.

(4) Hodge, E. S.; "Hot Isostatic Pressing Improves Powder Metallurgy Parts", Materials in Design Engineering, p 92; May 1965.

(5) Muzzall, C. E.; Compendium of Gas Autoclave Engineering Studies, Y-1478; Union Carbide Corporation-Nuclear Division, Y-12 Plant, Oak Ridge, Tennessee; August 23, 1965.

(6) Hall, H. T.; "Some High-Pressure High-Temperature Apparatus Design Considerations: Equipment for Use at 100,000 Atmospheres and 3000° C", Rev Sci Inst, 29, (4), p 267; April 1958.

(7) Hall, H. T.; "Ultra-High-Pressure, High-Temperature Apparatus: The Belt", Rev Sci Inst, 31, (2), p 125; February 1960.

(8) Hall, H. T.; "Ultra High Pressures", Sci Am, 201, (5), p 61; November 1959.

(9) Levey, R. P.; The Cold Pressing of Sinterable UO_2, Y-1340, Union Carbide Corporation-Nuclear Division, Y-12 Plant, Oak Ridge, Tennessee; June 1, 1961.

(10) French, D. W. and Thomas, D. A.; Hardness, Anisotropy, and Slip in Tungsten Carbide Crystals, Paper Presented to the AIME; October 1964.

(11) Schwarzkopf, P. and Kieffer, R.; Cemented Carbides; MacMillan Company (1960).

(12) Burch, Francis; "Thermoelectric Measurement of High Temperatures in Pressure Apparatus", Rev Sci Inst, 10, p 137; April 1939.

(13) Stoever, H. J.; Applied Heat Transmission; McGraw-Hill, New York (1941).

(14) Francl, J. and Kingery, W. D.; "Phase Equilibria at High Temperatures in Iron Silicate Systems", J Am Cer Soc, 37, pp 81-84 (1954).

(15) McQuarrie, M.; "Kiln Car Bearing Lubricants", J Am Cer Soc, 37, pp 85-88 (1954).